

X-rays and virtual taphonomy resolve the first *Cissus* (Vitaceae) macrofossils from Africa as early-diverging members of the genus¹

Neil F. Adams^{2,3,10}, Margaret E. Collinson^{2,4}, Selena Y. Smith⁵, Marion K. Bamford⁶, Félix Forest⁷, Panagiota Malakasi⁷, Federica Marone⁸, and Dan Sykes^{9,11}

PREMISE OF THE STUDY: Fossilized seeds similar to *Cissus* (Vitaceae) have been recognized from the Miocene of Kenya, though some were previously assigned to the Menispermaceae. We undertook a comparative survey of extant African *Cissus* seeds to identify the fossils and consider their implications for the evolution and biogeography of *Cissus* and for African early Miocene paleoenvironments.

METHODS: Micro-computed tomography (μ CT) and synchrotron-based X-ray tomographic microscopy (SRXTM) were used to study seed morphology and anatomy. Virtual taphonomy, using SRXTM data sets, produced digital fossils to elucidate seed taphonomy. Phylogenetic relationships within *Cissus* were reconstructed using existing and newly produced DNA sequences for African species. Paleobiology and paleoecology were inferred from African nearest living relatives.

KEY RESULTS: The fossils were assigned to four new *Cissus* species, related to four modern clades. The fossil plants were interpreted as climbers inhabiting a mosaic of riverine woodland and forest to more open habitats. Virtual taphonomy explained how complex mineral infill processes concealed key seed features, causing the previous taxonomic misidentification. Newly sampled African species, with seeds most similar to the fossils, belong to four clades within core *Cissus*, two of which are early diverging.

CONCLUSIONS: Virtual taphonomy, combined with X-ray imaging, has enabled recognition of the first fossil *Cissus* and Vitaceae from Africa. Early-divergent members of the core *Cissus* clade were present in Africa by at least the early Miocene, with an African origin suggested for the *Cissus sciaphila* clade. The fossils provide supporting evidence for mosaic paleoenvironments inhabited by early Miocene hominoids.

KEY WORDS *Cissus*; Hiwegi Formation; liana; *Menispermicarum*; microCT; Miocene; paleoecology; seeds; SRXTM; virtual taphonomy

¹ Manuscript received 26 April 2016; revision accepted 24 August 2016.

² Department of Earth Sciences, Royal Holloway University of London, Egham, Surrey, TW20 0EX, UK;

³ Department of Geography, Royal Holloway University of London, Egham, Surrey, TW20 0EX, UK;

⁴ Department of Earth Sciences, Natural History Museum, London, SW7 5BD, UK;

⁵ Department of Earth & Environmental Sciences and Museum of Paleontology, University of Michigan, Ann Arbor, Michigan 48109 USA;

⁶ Evolutionary Studies Institute and School of Geosciences, University of the Witwatersrand, P. Bag 3, Wits 2050, Johannesburg, South Africa;

⁷ Jodrell Laboratory, Royal Botanic Gardens, Kew, Richmond, Surrey, TW9 3DS, UK;

⁸ Swiss Light Source, Paul Scherrer Institut, CH-5232 Villigen, Switzerland; and

⁹ Imaging and Analysis Centre, Natural History Museum, London, SW7 5BD, UK

¹⁰ Author for correspondence (e-mail: Neil.Adams.2012@live.rhul.ac.uk)

¹¹ Present affiliation: School of Materials, University of Manchester, Oxford Road, Manchester, M13 9PL, UK
doi:10.3732/ajb.1600177

The volcanic and clastic sediments of the Hiwegi Formation on Rusinga Island, Lake Victoria, Kenya have yielded a rich early Miocene flora and fauna with well over 100 recorded species, dated to ca. 18–20 Ma (Drake et al., 1988; Andrews et al., 2009; Peppe et al., 2011). The floral assemblage contains fossilized fruits, seeds, twigs, wood, bark, and leaves (Chesters, 1957; Collinson et al., 2009; Maxbauer et al., 2013; Michel et al., 2014), and the faunal assemblage comprises numerous fossil mammals (e.g., Whitworth, 1958; Pickford, 1981; Butler, 1984; Werdelin, 2011), reptiles (e.g., Clos, 1995; Conrad et al., 2013), birds (e.g., Harrison, 1980; Rich and Walker, 1983) and invertebrates (e.g., Leakey, 1952; Verdcourt, 1963; Thackray, 1994; Pickford, 1995). The fauna also contains several genera of early hominoids (e.g., Le Gros Clark and Leakey, 1951; Andrews and Simons, 1977; Walker and Teaford, 1988; Walker et al., 1993; Harrison, 2002; McNulty et al., 2007; Harrison and Andrews, 2009; Pickford et al.,

2009), including *Ekembo* (previously *Proconsul*, see McNulty et al., 2015), which mark the transition between Paleogene arboreal primates, thought to inhabit tropical forests (Andrews, 1992; Janis, 1993), and Neogene bipedal hominoids, often associated with open savanna grassland (Robinson, 1963; Reed, 1997; Pickford, 2002). Study of the Hiwegi Formation flora is essential to understand the paleoenvironments in which these transitional hominoids evolved.

The fruit and seed flora was partly described by Chesters (1957) from surface-picked collections, but these lacked a sedimentological and stratigraphic context. These issues of specimen provenance prompted in situ excavations at the new site of R117 (Collinson et al., 2009), where over 360 fruits and seeds were collected, including several specimens tentatively identified as cf. *Cissus* sp. 1 nov. (Vitaceae). During that study, three other morphotypes with similarity to seeds of extant *Cissus* L. species were recognized among the collections originally studied by Chesters (1957, 1958). If these four fossil records of *Cissus* can be verified, they would constitute the first records of the Vitaceae in the flora, the earliest reported record of Vitaceae from the African continent and could provide evidence for arid- or rainforest-adapted taxa in the African Miocene vegetation (De Santo et al., 1987; Verdcourt, 1993; Lombardi, 2000; Manchester et al., 2012a).

Recent molecular phylogenetic analyses of the genus *Cissus* (Liu et al., 2013; Rodrigues et al., 2014) showed that modern species could be assigned to several distinct clades. All African species fell within the core *Cissus* clade, but within that were distributed in more than seven distinct subclades, two of which also included Asian species (Liu et al., 2013). However, many African species were missing from these phylogenies, including those with external seed morphology most similar to the putative *Cissus* fossils. If the fossils are *Cissus*, molecular study of these neglected modern species will be essential to place them in their phylogenetic context.

This paper therefore aims to (1) confirm or refute the identification of Hiwegi Formation fossils to *Cissus* and, if confirmed, identify the clades to which the fossil species are likely related by comparing external and internal seed morphology of the fossils to extant African species; (2) place the nearest living relatives of the fossils into the existing phylogenetic framework; and (3) evaluate the fossils' paleoenvironmental and biogeographic significance.

MATERIALS AND METHODS

Specimens studied—The fossil fruits and seeds from the Hiwegi Formation are composed of carbonate minerals, which derive from highly alkaline ash erupted from the nephelinite-carbonatite Kisingiri volcano during the Miocene (Bestland et al., 1995; Harris and Van Couvering, 1995), and which replaced biological structures during fossilization (Collinson et al., 2009). The specimens were collected from the Hiwegi Formation (for wider stratigraphic context, see Drake et al., 1988; Collinson et al., 2009) by surface-picking and in situ excavation and are stored in collections at the Natural History Museum, London (NHMUK, specimen numbers prefixed V) and the National Museums of Kenya, Nairobi (KNM). Three fossil seed morphotypes in NHMUK, which Chesters (1957, 1958) had placed in the Menispermaceae (due to their bisymmetry, horseshoe-shaped curvature, and sculptured margins), were noted by M. E. Collinson (personal observations) to have strikingly similar exterior seed coat morphology to modern African *Cissus* species, as illustrated in African floras (e.g., Dewit and Willems, 1960; Descoings, 1967, 1972;

Verdcourt, 1993). Collinson et al. (2009) also listed several specimens from the R117 site assigned to 'cf. *Cissus* sp. 1 nov.' (Vitaceae) based on similarity to modern *Cissus* seeds. All these fossils were re-examined during the current study.

Fifteen modern species of African *Cissus* and three species of African *Cyphostemma* (Planch.) Alston, which have comparable seed ornamentation to the putative *Cissus* fossils, were sampled from loose fruits on herbarium sheets in the Royal Botanic Gardens, Kew Herbarium (K) to study seed anatomy. The most visibly mature and undamaged specimens were selected. Additionally, fruits of *Cissus dasyantha* were obtained from the herbarium at the Botanic Garden Meise, Belgium (BR). Herbarium sheet information for the species sampled is provided in Appendix S1 (see Supplemental Data with the online version of this article).

Macrophotography and VP-SEM—Photographs of the specimens described by Chesters (1957, 1958) were provided by the NHMUK Photographic Unit. The smaller specimens, assigned to 'cf. *Cissus* sp. 1 nov.' by Collinson et al. (2009), were examined uncoated under a Leo 1455 vapor pressure scanning electron microscope (VP-SEM) at the Imaging and Analysis Centre, NHMUK. Specimens were placed loose onto a sheet of black paper in a small tray, moved into appropriate orientation and turned over using a fine (size 00000) artist's brush. A small amount of Blu-Tack (Bostik, Paris, France) was used, when unavoidable, to orient specimens for apical and basal views. Images were obtained using the back scatter detector (BSD), a chamber pressure of 14–15 Pa, current of 20 kV, spot size 500, and working distance 38–39 mm. Images were adjusted uniformly for contrast and brightness using Adobe (San Jose, California, USA) Photoshop CS2 or CS6.

Synchrotron-based X-ray tomographic microscopy (SRXTM)—The traditional method of boiling and scrubbing modern fruits to study their seeds is problematic. Depending on tissue toughness, seed features may not be revealed in a repeatable or comparable manner across different species or genera. Cutting or histological sectioning to study internal anatomy also has limitations: it is destructive, may introduce artifacts (tears, gaps), and multiple planes of section through the same specimen cannot be acquired. X-ray imaging solves these problems because multiple planes of section through a single specimen can be easily and nondestructively obtained (e.g., Smith et al., 2009). Modern *Cissus* and *Cyphostemma* fruits were scanned using SRXTM, as this technique provides the necessary quality of resolution to enable distinction of cellular details in the fruit wall and seed coat layers for systematic study and for virtual taphonomy (Smith et al., 2009; Collinson et al., 2013). The SRXTM was performed on the TOMCAT beamline at the Swiss Light Source, Paul Scherrer Institut, Villigen, Switzerland (Stampanoni et al., 2006). Specimens were mounted onto brass pin stubs using polyvinyl acetate glue and were scanned during one session of beamtime in July 2014. X-rays transmitted by the specimens were converted into visible light by a 300 μm -thick Ce-doped LAG scintillator screen. A microscope objective of 1.25 \times or 2 \times (depending on fruit size) magnified the projection data, which were then digitized by a high-resolution scientific CMOS camera (PCO.edge; PCO GmbH, Kelheim, Germany), giving a resultant voxel size of 3 to 5 μm . The energy was set at 17.5 keV, and the exposure time per projection was 50 ms. For each scan, 1501 projections (2560 \times 2160 pixels with PCO.edge camera) were acquired over 180°. Reconstruction algorithms were then used to combine the projections

and obtain a three-dimensional volume, reconstruction was performed on a dedicated Linux PC cluster using a highly optimized routine based on the Fourier transform method and a gridding procedure (Marone et al., 2010; Marone and Stampanoni, 2012). Multiple stacked scans were used if the specimens did not completely fit within the field of view. Three-dimensional data sets were visualized, and images and videos were captured, in the program Avizo 8.1 (FEI Visualization Science Group, Bordeaux, France). Images were adjusted uniformly for contrast and brightness using Adobe Photoshop CS2 or CS6. Videos of digital SRXTM tomograms in transverse section (DTS) through fruits of each of these modern species are available from the Dryad Digital Repository (<http://dx.doi.org/10.5061/dryad.g9r36>).

Micro-computed tomography (μ CT)—Externally visible ventral infolds are a characteristic feature of *Cissus* seeds (Chen and Manchester, 2011), but are not evident in the fossils (Fig. 1). Information on internal structure of the fossils (including holotypes) is required to test whether these characteristic ventral infolds are (1) genuinely absent, which would exclude affinity with Vitaceae; (2) present but externally obscured by a seed coat layer, which would indicate affinity with *Cyphostemma* (Chen and Manchester, 2011); or (3) obscured as a consequence of taphonomic processes, such as mineral infilling during fossilization, which would support identification to *Cissus*. For holotypes and rare fossils, this information must be obtained nondestructively. Therefore, three fossil specimens (V33753, V68501, V68506) from collections studied by Chesters (1957, 1958) and stored in NHMUK and two specimens (R117.1981.314, R117.1981.476) from the R117 site, identified by Collinson et al. (2009) as ‘cf. *Cissus* sp. 1 nov.’ and housed in KNM were scanned by μ CT using a Nikon Metrology HMX ST 225 at the Imaging and Analysis Centre, NHMUK. Specimens were stabilized by inserting them into blocks of OASIS Floral Foam (Smithers-Oasis Company, Kent, Ohio, USA) within in a plastic tube. Specimens were wrapped for protection in cling film: a thin film of PVC (polyvinyl chloride) or LDPE (low density polyethylene). A voltage of 200 kV was used with a current of 180 μ A, a tungsten reflection target, a 0.5 or 0.25 mm copper filter and an exposure time of 708 ms, resulting in a voxel size of 12 μ m. Four modern *Cissus* fruits scanned by SRXTM (one *C. dinklagei*, one *C. populnea*, two *C. integrifolia*) were also scanned using μ CT. This duplicative scanning aimed to ensure that μ CT scans of the fossils could be interpreted in the context of directly comparable scans of modern seeds (a comparison of imaging methods is provided in Appendix S2 with the online Supplemental Data). A voltage of 125 kV was used with a current of 200 μ A, a molybdenum reflection target, no filter and an exposure time of 708 ms, resulting in a voxel size of 8 to 15 μ m. μ CT data sets were reconstructed using CT Pro (Nikon Metrology, Tring, UK) and were visualized in Avizo 8.1. Images and videos were obtained as for SRXTM data sets. Videos are available from the Dryad Digital Repository (<http://dx.doi.org/10.5061/dryad.g9r36>).

Virtual taphonomy—The technique of virtual taphonomy, developed by Smith et al. (2009), solves the problem of potential variability in tissue removal with traditional boiling or scrubbing methods in seed preparation. Virtual taphonomy uses X-ray data sets to digitally remove specific tissue or cell layers from modern fruits or seeds, thereby creating digital fossils, the surfaces of which can be directly compared with real fossils to determine which layers are preserved. Digital seed infills can also be produced using this technique,

mimicking the mineral infill of fruits and seeds that can occur during fossilization (Smith et al., 2009; Collinson et al., 2013). For modern *Cissus populnea* Guill. & M.Brandt, a digital infill of the space inside the inner seed coat (the endotesta) was produced (a virtual fossil), to mimic mineral infill during fossilization. The ventral infolds were then digitally infilled to mimic processes that might have led to mineral obscuring the ventral infolds during fossilization.

Molecular phylogeny—Phylogenetic relationships within *Cissus* and the placement of species assigned to this genus within Vitaceae were assessed using available sequence data from the plastid genome (*trnL* intron, *trnL-F* spacer, *atpB-rbcL* spacer, *trnC-petN* spacer and *rps16* intron), as well as newly produced sequences of *trnL-F* and *rps16* for eight African *Cissus* species with seeds most similar to the putative *Cissus* fossils, which were not represented in previous molecular phylogenetic studies (see Appendix 1). Sequence data obtained from public repositories comprise 91 *Cissus* species and 92 species from other genera of Vitaceae (see Appendix 2).

Total genomic DNA was extracted using a standard CTAB-based protocol (Doyle and Doyle, 1987) and purified using a combined cesium chloride/ethidium bromide gradient and dialysis procedure. The *trnL* intron/*trnL-F* spacer and the *rps16* intron were amplified using the primers designed by Taberlet et al. (1991) and Shaw et al. (2005), respectively. Further details regarding the polymerase chain reactions, amplification procedures, PCR product purifications, and cycle sequencing reactions are provided in online Appendix S3.

Matrices (including sequences obtained from public repositories and those produced for the current study) were aligned using MUSCLE (Edgar, 2004) in the program Geneious; alignments are available from the TreeBASE depository (<https://treebase.org>; study ID 18491). A phylogenetic analysis was performed on a combined matrix using the maximum likelihood criterion as implemented in the program RAxML v8.1.24 (Stamatakis, 2014) using the rapid bootstrap algorithm with 1000 replicates and a search for the best-scoring tree. Divergence time estimates were obtained using the Bayesian inference approach implemented in the package BEAST v.1.8.2 (Drummond and Rambaut, 2007). All analyses were run on the Cipres Science Gateway portal (www.phylo.org). Further details of the phylogenetic analyses are provided in Appendix S3.

Calibration was performed using three fossils. The first is the oldest known fossil securely identified to the Vitaceae family (*Indovitis*) from the latest Cretaceous/earliest Paleogene Deccan traps of India (ca. 66 Ma, based on radiometric dating and biostratigraphy; Manchester et al., 2013) and was used as calibration on the crown node of subfamily Vitoideae (calibration A), comprising all genera of Vitaceae except the genus *Leea*, which is assigned to subfamily Leeoideae. A log-normal distribution was used, which allows the age to vary (given the uncertainty in fossil age estimation and given that a fossil's age is considered a minimum age for a given group), with an offset value of 65 and a standard deviation of 1.0. The second calibration point comes from fossil seeds assigned to *Ampelocissus parvisemina* Chen & Manchester from the late Paleocene of North America at the Beicegel Creek locality of the Sentinel Butte Formation, Fort Union Group, North Dakota (Chen and Manchester, 2007), considered by Zetter et al. (2011) to be late Paleocene (61.7–56.8 Ma) in age based on molluscan and mammalian (Kihm and Hartman, 1991; Hartman and Kihm, 1995) biostratigraphy and pollen zonation (Nichols and Ott, 1978). It was assigned to the stem node of the clade comprising genera *Ampelocissus* Planch., *Nothocissus* (Miq.) Latiff, *Parthenocissus* Planch., *Pterisanthes* Blume, *Vitis*



TABLE 1. Seed morphotypes of selected single-seeded, modern African *Cissus* species based on internal and external morphology obtained from synchrotron X-ray data sets and descriptions and illustrations in floras (Dewit and Willems, 1960; Descoings, 1972; Verdcourt, 1993). H = height, W = width.

Seed morphotype	Species	Description
1 (Figs. 6D, 6E, 7A)	<i>C. integrifolia</i> ; <i>C. populnea</i>	<ul style="list-style-type: none"> • Two-layered, thick fruit wall, with a denser outer layer and more porous inner layer • Seeds laterally flattened (height/width [H/W] ratio of 1.5–1.8 in median digital transverse section [DTS]), elongate in the dorsiventral dimension • Obvious break in seed coat near the chalaza • Outer endotesta consists of thin layer with different X-ray attenuation (possibly high mineral content) • Dense and thin seed coat • Seed surface with two marginal ridges, one on each lateral face, a ridged and faceted marginal area, long ridges radiating from ventral margin across lateral faces
2 (Figs. 6B, 7B)	<i>C. barbeyana</i> ; <i>C. dasyantha</i>	<ul style="list-style-type: none"> • Thin to moderately thick fruit wall • Seeds slightly laterally flattened (H/W ratio of 1.3–1.5 in median DTS), elongate in the dorsiventral dimension • Indistinct break in seed coat near the chalaza • Endotesta has uniform X-ray attenuation • Dense and moderately thick seed coat • Seed surface with two marginal ridges; a ridged and faceted marginal area, where ridges sometimes fuse to form a reticulum; short ridges radiating across part of the lateral faces
3 (Figs. 6H, 7C)	<i>C. lebrunii</i> ; <i>C. sciaphila</i> ; <i>C. tiliifolia</i>	<ul style="list-style-type: none"> • Thin fruit wall • Seeds not, or slightly, laterally flattened (H/W ratio of 1.0–1.6 in median DTS), short in the dorsiventral dimension • Indistinct break in seed coat near the chalaza • Endotesta has uniform X-ray attenuation • Thin seed coat of variable texture • Seed surface covered in ridges, forming a complete to incomplete reticulum across the lateral faces
4 (Figs. 6M, 7D)	<i>C. petiolata</i>	<ul style="list-style-type: none"> • Thick fruit wall • Seeds laterally flattened (H/W ratio of 1.5–1.8 in median DTS), short in the dorsiventral dimension • Thickened chalaza with no break in seed coat • Endotesta has uniform X-ray attenuation • Dense and thick seed coat • Seed surface smooth

L., and Yua C.L.Li, following Nie et al. (2012) and Liu et al. (2016) (calibration B). As for the previous calibration, a log-normal distribution was used, with an offset value of 55.8 and a standard deviation of 1.0. The third calibration point is the oldest fossil unequivocally assigned to genus *Cissus*, from the Belén flora (North Coastal Peru) of the Oligocene, with a maximum age of 30–28.5 Ma based on diatom biostratigraphy (Manchester et al., 2012a). This fossil has features shared with species from morphotype 1 and the *Cissus integrifolia* clade (see below); it was therefore assigned to the stem node of this group (calibration C) with a log-normal distribution with an offset value of 27.5 and a standard deviation of 1.0.

Extant *Cissus* seed morphological information—In addition to the 16 SRXTM data sets of African *Cissus* seeds most similar to the Hiwegi Formation fossils, published seed illustrations and

descriptions were sourced, where available, for all African *Cissus* species included in the molecular phylogeny (Table 1; online Appendix S4). Together, these data were used to determine the modern species with seeds most similar to those of the fossils and to place these nearest living relatives into the existing phylogenetic framework.

Ecological and biogeographic information—Data on the habit, habitat, and biogeographic distributions of extant *Cissus* species were gathered for extant species in clades containing similar seed morphotypes to the fossils (Table 2). Georeferenced occurrence data from illustrated herbarium sheets were obtained from the Global Biodiversity Information Facility (GBIF, 2013), and floras and other herbarium sheets were also used. Herbarium sheet sources are given in online Appendix S5.

FIGURE 1 External morphology of fossilized *Cissus* seeds from the Hiwegi Formation, Rusinga Island, Kenya. (A) Lateral, (B) apical, (C) basal, (D) ventral views of the *Cissus crenulata* (Chesters) comb. nov. holotype (V33753). (E) Ventral, (F) lateral, (G) apical, (H) basal views of the *Cissus andrewsii* sp. nov. holotype. (I) Lateral and (J) basal views of a paratype of *C. andrewsii* (V68500), and (K) lateral and (L) apical views of another paratype (V68502), demonstrating intraspecific variation in seed size, shape, ornamentation and basal/apical width. (M) Lateral, (N) basal and (O) apical views of the *Cissus rusingensis* sp. nov. holotype (R117.1981.314). (P, S, V) Lateral, (Q, T, W) basal and (R, U, X) apical views of paratypes of *C. rusingensis* (R117.1981.476, R117.1981.604, R117.1981.605 respectively), illustrating intraspecific variation in seed shape (subrounded to pyriform), the number of muri and enclosed lumina, the extent of the perichalazal rib and the length of the basal projection. (Y) Lateral, (Z) apical, (AA) basal, (BB) ventral views of the *Cissus psilata* sp. nov. holotype (V68506). Scale bar = 10 mm, in 1 mm increments.

TABLE 2. Distribution, habit, and habitat data of modern *Cissus* species.

Species	Distribution	Habit	Habitat	Sources
<i>C. adnata</i> Roxb.	Australasia; E, SE, and S Asia	Scrambling or climbing shrub, or woody liana, up to 10 m	Primary lowland monsoon forests, riparian forest, disturbed and semiopen scrub and deciduous forest, shrubland and thickets	1–4
<i>C. albiporcata</i> Masinde & L.E.Newton	E Africa	Climber	Bushland in rocky areas	3, 5
<i>C. aphyllantha</i> Gilg	E Africa	Shrub, scrambler or woody climber, 1–4 m tall	<i>Acacia</i> scrub or desert thornbush, scrubby woodland, rocky outcrops	3, 5
<i>C. aralioides</i> (Welw. ex Baker) Planch.	C, E and W Africa	Vigorous, succulent liana or herbaceous climber, a strong, lofty climber, up to 25 m	Coastal and riverine evergreen forest, rainforest, coastal bushland, <i>Acacia</i> bushland, grassland, thickets	3, 5–9
<i>C. barbeyana</i> De Wild. & T.Durand	C and W Africa	Herbaceous to woody, low, small liana	Rainforest, forest clearings, forest fragments and clusters	3, 6, 7, 9
<i>C. cactiformis</i> Gilg	E and S Africa	Succulent climber or scrambler, 1.2–4.5 m long	Woodland, mixed bushland, usually in stony places, rock domes	3, 5
<i>C. dasyantha</i> Gilg & M.Brandt	W Africa	Liana, up to 6 m	Occasionally flooded forest, gallery forests	3, 7
<i>C. faucicola</i> Wild & R.B.Drumm.	E Africa	Herbaceous climber, several meters long	Evergreen rainforest, especially edges by waterfalls and in grassy clearings	5, 8
<i>C. floribunda</i> (Baker) Planch.	E Africa	Thin, woody liana or climber, several meters long	Rainforest, dense moist tropical forest, disturbed forest or forest edge	4, 10
<i>C. integrifolia</i> (Baker) Planch.	C and E Africa	Herbaceous vigorous climber to 5 m, reaching tops of trees or thicket-forming	Evergreen riverine forest, woodland, bushland and savanna grassland, often on rocky scarps	3, 5, 7, 8, 11
<i>C. lebrunii</i> Dewit	C Africa	Herbaceous climber	Rainforest	3, 7
<i>C. oliveri</i> (Engl.) Gilg ex Engl.	C and E Africa	Herbaceous to woody climbing shrub, up to 6 m long	Riverine and gallery forest, marshy areas, papyrus swamps, wet grassland with scattered trees	3, 5, 7
<i>C. oreophila</i> Gilg & M.Brandt	C and W Africa	Large herbaceous liana	Gallery and riverine forest, forest edges, swamp areas	3, 4, 6, 9
<i>C. petiolata</i> Hook.f.	C, E and W Africa	Large, somewhat succulent liana, vigorous climber or scrambler, to at least 10 m	Riverine forest, occasionally flooded forest edges, thickets, <i>Acacia</i> mixed bushland, rocky ground with scattered trees and shrubs, woody/shrub savanna	3, 5–9, 11
<i>C. phymatocarpa</i> Masinde & L.E.Newton	E Africa	Climber	Thickets on forest edges and coastal bushland	3, 5
<i>C. polita</i> Desc.	E Africa	Herbaceous liana, 1.5–3 m	Calcareous hills and plateaux; dry, deciduous seasonal forest; savanna grassland with dry forest	4, 10
<i>C. polyantha</i> Gilg & M.Brandt	C, E and W Africa	Herbaceous to woody climber/liana, up to 15 m	Riverine and gallery rainforest, rocky hollows in grassland and thickets	3, 5–7, 9
<i>C. populnea</i> Guill. & Perr.	C, E and W Africa	Bushy liana, to 4.5 m	Wooded savanna, rocky outcrops and scree, bushland, lowland forest edges	3, 5–7, 9
<i>C. pseudoguerkeana</i> Verdc.	E Africa	Spreading herb, at least 60 cm long	Woodland, low shrubs on sand, swampy places	3, 5
<i>C. quadrangularis</i> L.	Arabia; C, E, N, S, and W Africa; SE and S Asia	Succulent bushy liana 1–15 m long, or succulent climbing shrub	Xerophilic thickets, thorny savanna, <i>Acacia</i> woodland, grassland, riverine thicket, coastal forest edges	3, 5, 8–10
<i>C. quarrei</i> Dewit	C and E Africa	Erect herb or herbaceous climber, 0.6–1 m tall	Riverine vegetation, <i>Brachystegia</i> woodland	3, 5, 7, 8
<i>C. rhodotricha</i> (Baker) Desc.	E Africa	Scrambling and climbing strong liana or erect shrub	Rocky outcrops, deciduous seasonal forest, wooded savanna	10
<i>C. rondoensis</i> Verdc.	E Africa	Herbaceous to semiwoody climber to around 4 m	Moist, (semi) evergreen forest, dense forest thicket	3–5
<i>C. rostrata</i> (Miq.) Korth. ex Planch.	SE Asia	Climber/liana, up to 10–15 m	Fringe and understorey forest; forest river banks, peat swamp/ marshy forest	3, 4, 12
<i>C. rotundifolia</i> Vahl	Arabia; C, E and S Africa	Succulent, herbaceous to woody, vigorous climber/liana, to 5 m	Dry woodland and bush, thorny savanna, <i>Acacia</i> scrub, bushland, thickets, dry forest and forest edges particularly on rocky outcrops	3, 5, 7, 8
<i>C. sagittifera</i> Desc.	E Africa	Creeping or climbing, thin liana	Woodland edges, limestone cliffs, quartzite outcrops	3, 4, 10
<i>C. sciaphila</i> Gilg	E Africa	Woody climber/liana, 3–12 m long or shrubby	Lowland riverine forest fringes, woodland slopes above river valleys	3, 5, 8
<i>C. smithiana</i> (Baker) Planch.	C and W Africa	Large liana/climber	Rainforest, forest galleries and edges	3, 7, 9
<i>C. sylvicola</i> Masinde & L.E.Newton	E Africa	Herbaceous, somewhat succulent and fleshy liana, to 12 m	Evergreen forest, also forest on rocky hills, coralline limestone and thicket	3, 5
<i>C. tiliifolia</i> Planch.	C and E Africa	Herbaceous to woody climber, up to 10 m	Forest and thickets in swampy areas, particularly near lake shores, swampy grassland	3, 5
<i>C. welwitschii</i> (Baker) Planch.	C and E Africa	Vigorous, woody climber, 2–9 m long, or shrubby	Semievergreen bushland, riverine fringes, thickets and termite mounds in <i>Brachystegia</i> woodland, rocky outcrops	3, 5, 8

Sources: (1) Lu (1993); (2) Chen et al. (2007); (3) GBIF (2013); (4) herbarium sheet data (online Appendix S5); (5) Verdcourt (1993); (6) Keay (1958); (7) Dewit and Willems (1960); (8) Wild and Drummond (1966); (9) Descoings (1972); (10) Descoings (1967); (11) Beentje (1994); (12) Yeo et al. (2012).

SYSTEMATICS

Definitions of lateral, ventral, dorsal, apical, and basal views and seed height, width, and dorsiventral dimension are given in online Appendix S6.

Family—Vitaceae Juss. 1789.

Genus—*Cissus* L. 1753.

Species—*Cissus crenulata* (Chesters) Adams, Collinson, S.Y. Smith & Bamford comb. nov.

Basionym—*Menispermicarpum crenulatum* Chesters (1957, pl. 19, figs. 19, 20).

Emended diagnosis—Seed bilaterally symmetrical, 19 mm in dorsiventral dimension, laterally flattened, suboval to D-shaped in lateral view, narrowly elliptical and 7 mm wide in apical and basal views, and elliptical in ventral view. Center of lateral face crossed by four pronounced, long ridges radiating from adjacent to the ventral infolds; longest ridge almost as long as seed; curved ridge, 2–3 mm from dorsal and basal margins of lateral faces, delineates faceted marginal area; prominent median ridge (rib perichalaza) extends from beneath ventral infolds, around base, over dorsal margin, and almost full length of apical margin as far as ventral infolds. Upper portion of ventral surface concave, forming acute angle with long axis of seed; pair of very deep, narrow ventral infolds present.

Holotype—Seed: V33753 (Fig. 1A–D; μ CT DTS video available from the Dryad Digital Repository, <http://dx.doi.org/10.5061/dryad.g9r36>).

Excluded specimens—Seeds: KNMP-RU7787 (8 specimens with field number 60*52, formerly P. B. 8, designated as paratypes of *Menispermicarpum crenulatum* by Chesters, 1957).

Type locality—Rusinga Island, Lake Victoria, Kenya.

Geological horizon and age—Hiwegi Formation, early Miocene.

Repository—Natural History Museum, London, UK.

Description—The seed is bilaterally symmetrical around a prominent median perichalazal rib (Fig. 1B, C), laterally flattened with a height/width ratio of 1.7 (Fig. 1A, B), suboval to D-shaped in lateral view (Fig. 1A), 19 mm in the dorsiventral dimension and 11 mm in height, narrowly elliptical and 7 mm wide in apical (Fig. 1B) and basal (Fig. 1C) views, and elliptical in ventral view (Fig. 1D). The seed apex is rounded, with no indication of an apical notch or chalazal grooves (Fig. 1A–C), and the seed narrows to the ventral margin (Fig. 1A–C). The seed ornamentation is most clearly visible on one lateral face (Fig. 1A). A curved ridge, 2–3 mm from the basal and dorsal margins of the lateral faces, delineates a faceted outer margin with facets spaced at 2.5 to 4.5 mm (Fig. 1A). There are short ridges (ca. 2 mm long), roughly perpendicular to the long curved ridge, within the outer margin, which define the facets (Fig. 1A). There are at least four ridges crossing the center of the lateral face, with one long (10 mm) ridge perpendicular to the ventral surface, and three curved ridges, which radiate away from the ventral

surface toward the basal margin, abutting the curved ridge (Fig. 1A). The reverse lateral face is partly obscured by mineral encrustation in the holotype (the only specimen), making the ornamentation less clear. Nevertheless, at least three clearly distinguishable ridges cross the center of the face radiating from the ventral surface, with one longer and more pronounced than the others. In lateral view, the upper portion of the ventral surface is nearly straight for three-quarters of its length, but the basalmost part is indented, forming an angle of ca. 65° with the long axis of the seed (Fig. 1A). The seed narrows into a rounded point on the ventral surface, possibly equivalent to the beak in typical Vitaceae (see fig. 1 of Chen and Manchester, 2011). The lateral flattening, near-straight ventral surface and suboval, or near elliptical, outline give the seed a very different shape from typical Vitaceae genera (e.g., Chen and Manchester, 2011). Externally the ventral infolds are only tentatively identifiable from a pink mineral infill from the apical and ventral views (Fig. 1B, D). However, in μ CT digital transverse section (DTS), a pair of very deep (4.5 mm) and narrow (0.5 mm) ventral infolds are clearly delineated by a very thin gap (black in Fig. 2C) between the inferred outer surface of the endotesta and the mineral infill of the infolds (outlined in solid yellow in Fig. 2D).

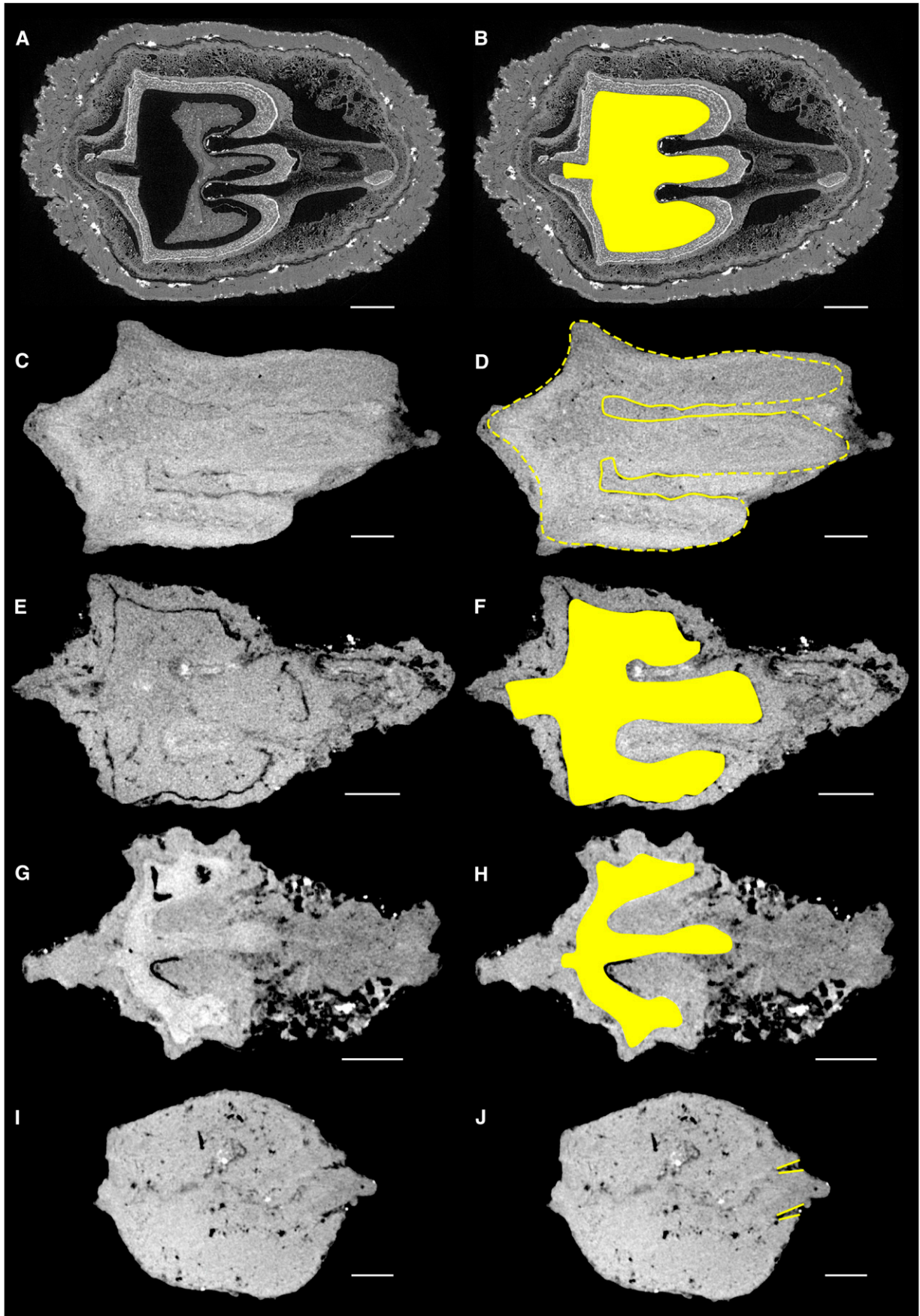
Comments—Seeds of modern *Cissus integrifolia* (Baker) Planch. are very similar to the holotype of *C. crenulata*, being narrow, laterally flattened and suboval in lateral view with a line of bisymmetry passing through a median longitudinal rib perichalaza and having a similar seed coat ornamentation. However, the greater number of ridges across the lateral faces and different orientation of the ventral surface relative to the long axis of the seed in *Cissus integrifolia* support the recognition of a separate species. Chesters (1957) listed P. B. 8 as a paratype of *Menispermicarpum crenulatum*. Currently, the number KNMP-RU7787 (P. B. 8) includes eight specimens, which have here been transferred to *Cissus andrewsii* sp. nov. (see below). Therefore, *Cissus crenulata* is represented only by a single specimen.

Species—*Cissus andrewsii* Adams, Collinson, S.Y. Smith, & Bamford sp. nov.

Etymology—The species epithet *andrewsii* is named in honor of Dr. Peter Andrews, in recognition of his extensive work on the Kenyan Miocene and the invaluable support he provided, which enabled one of us (Collinson) to undertake fieldwork on Rusinga and Mfangano Islands in 1980–1981.

Diagnosis—Seeds bilaterally symmetrical, 16–19 mm in dorsiventral dimension, laterally flattened, suboval in lateral view, narrowly elliptical and 5–8 mm wide in apical and basal views, elliptical in ventral view. Centers of lateral faces ornamented by 4–5 short ridges in radial pattern; curved ridge 1–2.5 mm from margins of lateral faces extends around most of seed and delineates faceted to reticulate marginal area; prominent median ridge (rib perichalaza) extends from base of ventral surface, around base, over dorsal surface, and almost full length of apical surface. Upper portion of ventral surface forms acute angle with long axis of the seed. Pair of deep, wide ventral infolds present.

Holotype hic designatus—Seed: V68501 (Fig. 1E–H; μ CT DTS video available from the Dryad Digital Repository, <http://dx.doi.org/10.5061/dryad.g9r36>).



Type locality—Rusinga Island, Lake Victoria, Kenya.

Paratypes—Seeds: V68500 (Fig. 1I, J); V68502 (Fig. 1K, L); KNMP-RU7787 (8 specimens with field number 60*52, formerly P. B. 8, previously listed as paratypes of *Menispermicarpum crenulatum* by Chesters, 1957; re-examined for this study by Bamford).

Geological horizon and age—Hiwegi Formation, early Miocene.

Repository—Natural History Museum, London, UK (holotype and paratype specimens with prefix V); National Museums of Kenya, Nairobi, Kenya (other paratypes).

Description—Seeds are bisymmetrical around a prominent median perichalazal rib (Fig. 1H, J) and vary from 16 to 19 mm in dorsiventral dimension, 11 to 15 mm in height and 5 to 8 mm in width (Fig. 1E–L). Seeds are laterally flattened with height/width ratios of 1.9–2.4 and are narrow in apical and basal views (Fig. 1G, H, J, L). The seed apex is rounded, with no indication of an apical notch or chalazal grooves (Fig. 1E–G), and narrows to the ventral margin (Fig. 1F, G). The ventral surface is slightly rounded, not straight (Fig. 1F, K). The lateral surfaces have a curved ridge, delimiting a sculptured outer margin, which extends from approximately half way along the apical margin, around the dorsal margin, and fully along the basal margin (Fig. 1F). The sculptured marginal band is faceted, facets spaced at 2 to 3.5 mm, and ridged with ridges sometimes fusing to form a reticulum (Fig. 1F, I, K). The central areas of the lateral faces are ornamented by four to five short (2–3 mm) ridges in a radial arrangement (Fig. 1F). Where undamaged, the upper portion of the ventral surface forms an angle of 52° to 55° with the long axis of the seed (Fig. 1F, K). The ventral infolds are not visible on the outside of the seed (Fig. 1E, G, L), but by using μ CT, deep (2.5 mm), broad (0.6 mm) ventral infolds can be identified in V68501 (Fig. 2F) by differences in X-ray attenuation (gray level) due to variation in mineral density and mineral texture in the infold infills. A very clear gap (black in Fig. 2E) demarcates the inferred original position of the endotesta outer surface in the areas away from the infolds, where endotesta would have been originally thicker based on observations in modern seeds. Some additional outer mineral (possibly representing exotesta or fruit wall remnants) is also present in the holotype (Fig. 2E).

Comments—In her unpublished thesis, Chesters (1958) assigned the specimen shown in Fig. 1E–H (V68501) to *Menispermicarpum crenulatum*, here revised to *Cissus crenulata*, but there are clear differences between *C. crenulata* and V68501, supporting assignment of this specimen, and other similar specimens, to a new species. Although there is now only a single specimen of *Cissus crenulata*

(making it impossible to assess intraspecific variation), there are 11 specimens of *C. andrewsii*, all with consistent morphology distinct from that of the single specimen of *C. crenulata*. In *Cissus andrewsii* the central portion of the lateral faces is crossed by short ridges in a radial pattern, unlike *C. crenulata*, and the lateral faces have a greater number of short transverse ridges in the outer margins, some of which fuse to form a reticulum. In addition, the curved ridge, delineating the sculptured margin from the central flat area, extends farther down the ventral surface and the ventral margin is curved not straight. *Cissus andrewsii* is therefore more similar to seeds of modern *Cissus dasyantha* Gilg & M.Brandt than *C. integrifolia*, but is sufficiently different from these extant species to warrant assignment to a new species, and differs in several ways from the fossil *C. crenulata*.

Species—*Cissus rusingensis* Adams, Collinson, S.Y.Smith, & Bamford sp. nov.

Synonymy—‘cf. *Cissus* sp. 1 nov.’ in Collinson et al. (2009).

Etymology—The epithet *rusingensis* refers to the type locality on Rusinga Island from which the specimens were collected during in situ excavations.

Diagnosis—Seeds bilaterally symmetrical, 7–8 mm in dorsiventral dimension, slightly laterally flattened, subrounded to pyriform in lateral view, broadly elliptical in apical, basal, and ventral views. Lateral faces ornamented by ridges and reticula with 7–11 wide muri radiating to margins and enclosing lumina in central area; prominent median ridge (rib perichalaza) extends from ventral margin, around base, over dorsal surface, and almost full length of the apex. Upper portion of ventral surface forms acute angle with long axis of the seed. Pair of deep, very wide ventral infolds present.

Holotype hic designatus—Seed: R117.1981.314 (Fig. 1M–O; μ CT DTS video available from the Dryad Digital Repository, <http://dx.doi.org/10.5061/dryad.g9r36>).

Type locality—R117 site (see Collinson et al., 2009), Rusinga Island, Lake Victoria, Kenya.

Paratypes—Seeds: KNMP-RU9647 (field number R117.1981.422); R117.1981.476 (Fig. 1P–R; μ CT DTS video available from the Dryad Digital Repository, <http://dx.doi.org/10.5061/dryad.g9r36>); R117.1981.604 (Fig. 1S–U); R117.1981.605 (Fig. 1V–X).

Geological horizon and age—Grit Member, Hiwegi Formation, early Miocene.

FIGURE 2 Ventral infolds revealed in a seed of modern African *Cissus populnea* Guill. & Perr. (A, B) by synchrotron-based X-ray tomographic microscopy (SRXTM) and in fossil seeds from the Hiwegi Formation, Rusinga Island, Kenya (C–J), assigned to *Cissus* herein, by micro-computed tomography (μ CT). (A, B) SRXTM digital transverse section (DTS) through modern *C. populnea*, infill of the endotesta in yellow in (B) highlighting the position of the ventral infolds. (C, D) μ CT DTS through the holotype (V33753) of *Cissus crenulata* comb. nov., with (D) showing inferred position of the ventral infolds (solid yellow lines) and the margins of the endotesta (dotted yellow lines). (E, F) μ CT DTS through the holotype (V68501) of *Cissus andrewsii* sp. nov., with (F) showing infill of the inferred endotesta in yellow, highlighting two parallel, broad ventral infolds. (G, H) μ CT DTS through the holotype (R117.1981.314) of *Cissus rusingensis* sp. nov., with (H) showing infill of inferred embryo cavity within endotesta in yellow, highlighting two parallel, very broad ventral infolds. (I, J) μ CT DTS through holotype (V68506) of *Cissus psilata* sp. nov., with (J) showing inferred position of pair of very short, narrow parallel ventral infolds (solid yellow lines). All μ CT sections obtained from near ventral part of seeds, where ventral infolds were most likely to be evident, if concealed externally, based on their position in modern *Cissus* seeds. Scale bars = 1 mm.

Repository—National Museums of Kenya, Nairobi, Kenya (KNM).

Description—Seeds are bisymmetrical around a prominent median perichalazal rib (Fig. 1N, O, Q, R, T, U, W, X), and they vary from 7 to 8 mm in dorsiventral dimension, 5 to 6 mm in height, and 3 to 4 mm in width (Fig. 1M–X). The seeds are laterally flattened with a height/width ratio varying between 1.5 and 1.8 and are broadly elliptical in apical and basal views (Fig. 1N, O, Q, R, T, U, W, X). The seeds have a rounded apex (Fig. 1M, P, S, V) but are variable in their lateral shape (Fig. 1M, P). The perichalazal rib extends around less of the specimen in R117.1981.476 (Fig. 1P) and R117.1981.604 (Fig. 1S), resulting in a reduced lateral width higher up the seed, a longer ventral projection and a more pyriform shape. By contrast, the holotype (Fig. 1M) and R117.1981.605 (Fig. 1V) are both subrounded with only small ventral projections. The lateral surfaces have a reticulate ornamentation with one or two centrally positioned lumina (Fig. 1M, P, S, V) and 7 to 11 muri or ridges ranging in width from 0.2 to 0.6 mm (e.g., Fig. 1M). Some ridges radiate to the edges of the specimen and join up with the strong perichalazal rib producing marginal lumina (Fig. 1O, X). Others terminate before reaching the margin without forming a reticulum (bottom right in Fig. 1S; top left in Fig. 1V), resulting in a radiating pattern of marginal ridges and unenclosed marginal depressions. The upper portion of the ventral surface forms an angle of 35° to 55° with the long axis of the seed (Fig. 1M, P, S, V). The ventral infolds, although not externally visible (Fig. 1N, Q, T, W), are readily identifiable in the holotype by differences in contrast and mineral density in μ CT scans (Fig. 2G). A distinct pale area (highlighted yellow in Fig. 2H) marks the position of the embryo cavity, while the deep (1.5 mm) and very broad (0.75 mm) ventral infolds are infilled with mineral with lower X-ray attenuation and hence darker gray color (Fig. 2H).

Comments—*Cissus rusingensis* is distinctive in lacking a distinct curved ridge delineating a marginal region and in having muri in the central area of the lateral faces forming a reticulum. This species is very similar to seeds of modern *Cissus lebrunii* Dewit, but *C. rusingensis* has fewer muri and at most two (rather than three) centrally positioned lumina.

Species—*Cissus psilata* Adams, Collinson, S.Y. Smith, & Bamford sp. nov.

Etymology—The epithet *psilata* derives from the ancient Greek adjective *psilós*, meaning bare or smooth, and refers to the lack of seed coat ornamentation on the smooth surface of the lateral faces.

Diagnosis—Seed bilaterally symmetrical, 7.5 mm in dorsiventral dimension, subrounded in lateral view, broadly elliptical in apical, basal, and ventral views. Seed smooth, lacks external ornamentation (psilate), except for prominent median ridge (rib perichalaza) that extends all around dorsal surface, over apex, and almost full length of ventral surface. Base of ventral surface concave, forming acute angle with long axis of seed. Pair of very short, narrow ventral infolds present.

Holotype hic designatus—Seed: V68506 (Fig. 1Y–BB; μ CT DTS video available from the Dryad Digital Repository, <http://dx.doi.org/10.5061/dryad.g9r36>).

Type locality—Rusinga Island, Lake Victoria, Kenya.

Geological horizon and age—Hiwegi Formation, early Miocene.

Repository—Natural History Museum, London, UK.

Description—Seed inferred to be originally bilaterally symmetrical around a prominent median perichalazal rib, although the single specimen is slightly deformed (Fig. 1Z, AA), probably due to abnormal development in life or distortion during fossilization. The seed is subrounded in lateral view (Fig. 1Y), 7.5 mm in dorsiventral dimension and 6 mm in height, and broadly elliptical in apical and basal (Fig. 1Z, AA) views, 4.5 mm in width. The seed is not laterally flattened and has an inflated morphology with a height/width ratio of 1.3. The perichalazal rib is ca. 0.3–0.45 mm thick around the dorsal and basal margins (Fig. 1Y, Z) but thicker at the seed base (ca. 0.8 mm), forming a strong point (Fig. 1Y, AA), equivalent to the beak in typical Vitaceae (see fig. 1 of Chen and Manchester, 2011). The lateral surfaces are smooth (Fig. 1Y). The upper portion of the ventral surface forms an angle of 45° with the long axis of the seed (Fig. 1Y). The ventral infolds are not visible on the outside of the seed (Fig. 1Z, BB). μ CT scans of the holotype (Fig. 2I) show very little internal information compared to the other fossils, except for two very short (less than 0.5 mm) grooves at the base of the ventral surface (Fig. 2J), which correspond to the position of the ventral infolds characteristic of *Cissus*.

Comments—In her unpublished thesis, Chesters (1958) suggested that V68506 could be assigned to the genus *Menispermicarpum* as a new, but never published, species. However, the fossil morphology differs from endocarps of Menispermaceae. It is almost identical to seeds of modern *Cissus petiolata* Hook.f., differing in the greater extent of the rib perichalaza on the dorsal surface. In modern *Cissus petiolata* seeds, the ventral infolds are very shallow and short which, in combination with mineralization effects, can explain the very limited evidence for this diagnostic feature in V68506 (Fig. 2J).

RESULTS

Identification of fossils to genus *Cissus*—The lack of cellular and tissue detail in the fossils (Fig. 2C–J), and the complexities of mineralization during fossilization, make it difficult to judge if the external morphology of a fossil represents the external morphology of a living equivalent. The SRXTM videos of modern *Cissus* seeds (available from the Dryad Digital Repository, <http://dx.doi.org/10.5061/dryad.g9r36>) show that the inner and outer surfaces of the endotesta are parallel to one another, and hence, a mineral infill of the endotesta will have a very similar external morphology to a mineral replacement of the endotesta itself. Therefore, it is justifiable to compare the external surface of the Hiwegi Formation fossils with that of modern seeds for purposes of identification. These comparisons show that several modern African *Cissus* species have seeds with almost identical shape and ornamentation to the Hiwegi Formation fossil seeds (see *Phylogenetic context of seed morphotypes*). However, the ventral infolds that characterize modern *Cissus* seeds are not visible on the fossils. The taphonomy of the fossils may explain the absence of these key features.

A novel approach in virtual taphonomy was used to produce a digital infill of the endotesta of a modern *Cissus* seed (Fig. 3A). This virtual fossil showed all the key characteristics of *Cissus* seeds (i.e., a long, linear chalaza, the perichalaza; a thickened ridge of seed coat along the perichalaza, the perichalazal rib; deep, narrow, and linear

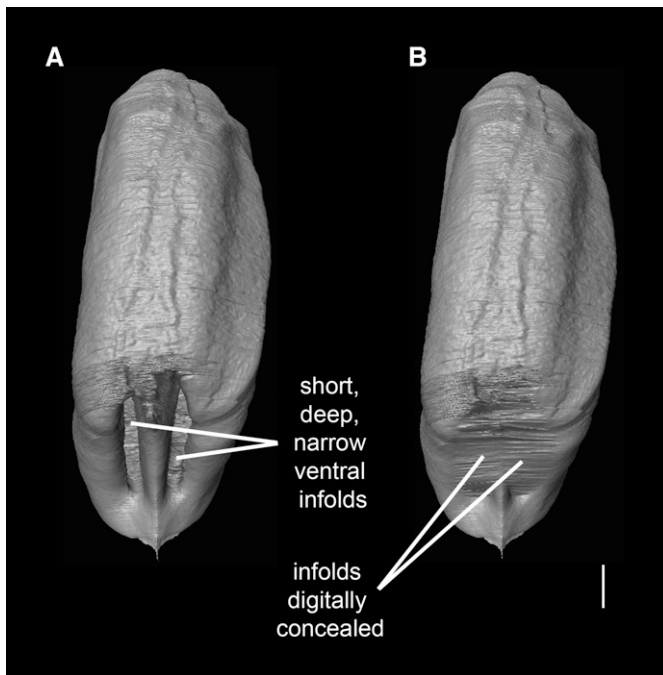


FIGURE 3 Virtual taphonomy using digital fossils produced from a synchrotron X-ray data set of a modern fruit of *Cissus populnea* Guill. & Perr. Specimen oriented in oblique ventral/apical view to best display ventral infolds. (A) Produced by digitally infilling space inside endotesta of seed, showing externally conspicuous pair of ventral infolds, thereby mimicking mineral seed infill processes during fossilization. (B) Produced by digitally concealing ventral infolds in (A) thereby mimicking taphonomic processes that could conceal ventral infolds by mineral infill. Scale bar = 1 mm.

ventral infolds). Digital infilling of the ventral infolds produced a digital fossil comparable to the real Hiwegi Formation fossils (Fig. 3B). This virtual taphonomy suggests a two-stage fossilization process with an initial infilling of the endotesta (and perhaps some mineral replacement of organic tissues) followed by a later stage of infilling of the ventral infolds. μ CT imaging supports this hypothesis because mineral-infilled ventral infolds can be recognized (Fig. 2C–J) in digital sections through the fossils (albeit more clearly in some specimens than others).

The only other modern genus including seeds similar to *Cissus* is *Cyphostemma*, some seeds of which may be laterally flattened and have somewhat similar ornamentation. Unlike *Cissus* (Fig. 4A) the ventral infolds on extant *Cyphostemma* seeds are externally concealed by extra layers of endotestal sclereids (Chen and Manchester, 2011; Fig. 4B). If the fossils were originally *Cyphostemma* seeds with the endotesta infilled by mineral during initial stages of fossilization, then the spaces enclosed by the endotesta over the ventral infolds would have been infilled at the same time as the main area within the endotesta. However, μ CT images of the fossils show mineral infills of the ventral infolds that are distinct from other mineral infill within the endotesta (Fig. 2C–H) indicating infill during a later stage of fossilization.

The combined data show that four African fossil seed morphotypes conform to the genus *Cissus* in all characters that can be determined from the fossils. The complex taphonomy and concealment of key features diagnostic of the genus explain the original taxonomic misidentification to the Menispermaceae.

Phylogenetic relationships within *Cissus*—In our maximum likelihood analysis, species of *Cissus* are found in three distinct groups (Fig. 5; online Appendix S7): the *Cissus striata* clade (bootstrap support [BS]/Bayesian posterior probabilities [PP] of 81%/0.94), the *Cissus trianae* clade (<50% BS/0.25 PP), and the core *Cissus* clade (60% BS/1.0 PP), as previously identified by Rodrigues et al. (2014). Within the core *Cissus* clade in our analysis, the early-diverging lineages comprise only African species (Fig. 5). The African species *Cissus barbeyana*, *C. sagittifera*, and *C. floribunda* form a clade (the *Cissus barbeyana* clade; 100% BS/1.0 PP) sister to the remainder of the core *Cissus* clade, in which the *Cissus integrifolia* clade (*C. integrifolia* + *C. populnea*; 100% BS/1.0 PP) is sister to two main clades that comprise the rest of the species in genus *Cissus*. In the first of these two main clades (100% BS/1.0 PP), only eight of 35 species in our analysis are not African; while only seven of the 49 species in the second clade are African (Fig. 5). The topologies and support values obtained with the maximum likelihood (Fig. 5) and Bayesian analyses (online Appendices S8–S10) do not present well-supported topological discrepancies. The divergence time analyses estimated that the core *Cissus* clade diverged 57.9 Ma (highest posterior density (HPD) 55.9–64.0 Ma; 95% HPD intervals of age estimates are provided in online Appendix S11), in the late Paleocene (online Appendix S8), and started to diversify 41.5 Ma (HPD 31.6–51.0 Ma), in the late middle Eocene (online Appendix S9).

Phylogenetic context of seed morphotypes—Seeds of four distinct *Cissus* species are now recognized from the early Miocene Hiwegi Formation. Given that claims of Vitaceae pollen from the Oligocene of Cameroon remain unconfirmed (Salard-Cheboldaeff, 1978, 1981; Muller, 1981), these seeds represent the first confirmed fossil record of Vitaceae and of the genus *Cissus* in Africa. The four fossil species represent distinct morphotypes, which are also found in seeds of extant species (Table 1), as revealed by SRXTM imaging of modern fruits and by a literature survey of published seed descriptions. The phylogenetic position of these extant species provides a phylogenetic context for the early Miocene fossils.

Morphotype 1—*Cissus crenulata* (Fig. 1A–E) has laterally flattened, subovate seeds with a faceted marginal area, several long radiating lateral ridges and two marginal ridges. The extant species *Cissus integrifolia* (Figs. 6D, 7A) and *C. populnea* (Figs. 2A, 6E) share this distinctive morphotype (Table 1). These two species are recovered in our phylogenetic analyses with strong support (100% BS) as a distinct clade, the *Cissus integrifolia* clade, which is one of the two earliest-diverging clades in core *Cissus* (Fig. 5). It is, therefore, likely that *Cissus crenulata* was a member of the early-diverging *Cissus integrifolia* clade.

Morphotype 2—*Cissus andrewsii* has seeds that are laterally flattened and have a ridged and faceted marginal area where ridges sometimes fuse to form a reticulum, two prominent marginal ridges, and short radiating lateral ridges. The extant species *Cissus barbeyana* (Fig. 6B) and *C. dasyantha* (Fig. 7B and fig. 13J) of Dewit and Willem, 1960) are most similar to *C. andrewsii*, in that they are slightly laterally flattened (height/width ratio of 1.3–1.5) with a similarly ridged and faceted marginal reticulum, two marginal ridges and short radiating lateral ridges (Table 1). Although the sampled specimen of *Cissus dasyantha* failed to amplify material for phylogenetic analysis, *C. barbeyana* was found in the basal clade of core *Cissus*, the *Cissus barbeyana* clade, with *C. floribunda* and *C. sagittifera*

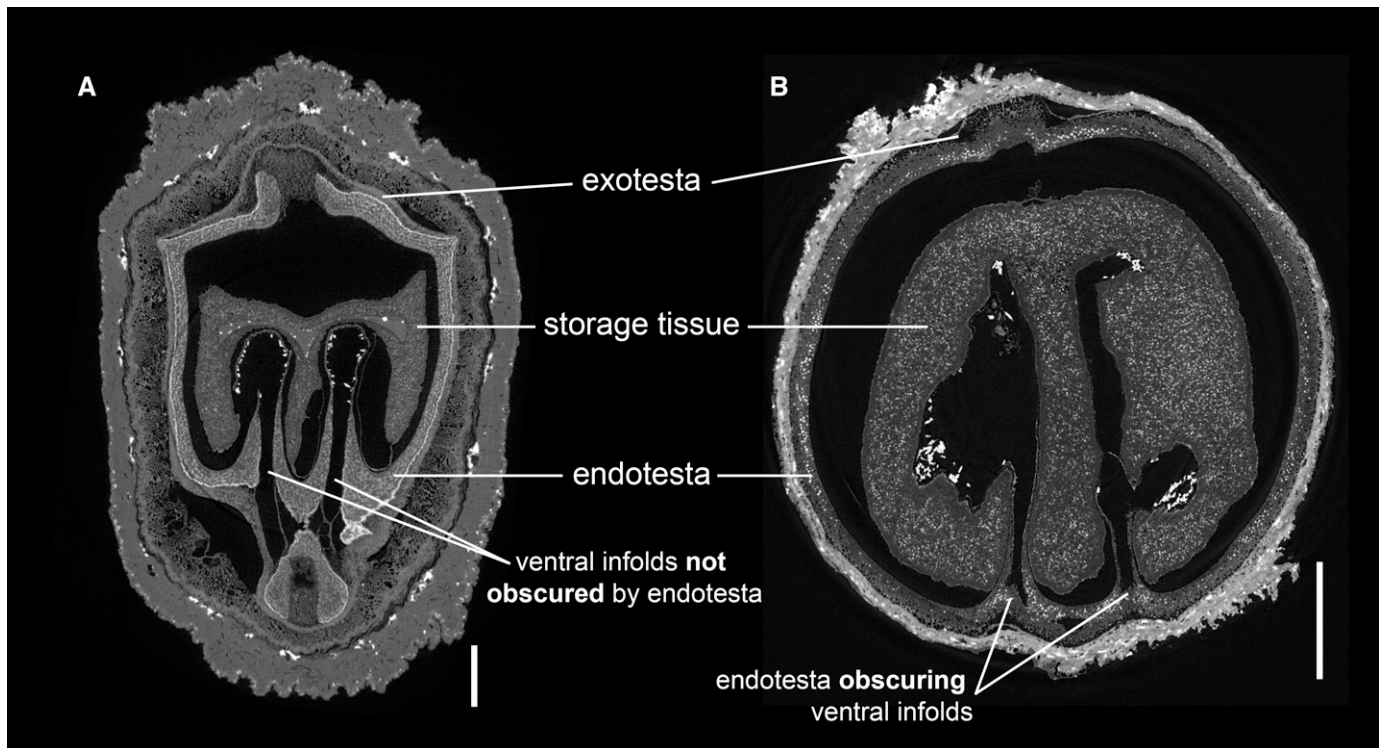


FIGURE 4 Comparative tissue organization in *Cissus* (A) and *Cyphostemma* (B) showing how the endotesta obscures ventral infolds in *Cyphostemma*. (A, B) Digital transverse sections, produced by synchrotron-based X-ray tomographic microscopy, through modern fruits. (A) *Cissus populnea* Guill. & Perr. (B) *Cyphostemma maranguense* (Gilg) Desc. Scale bars = 1 mm.

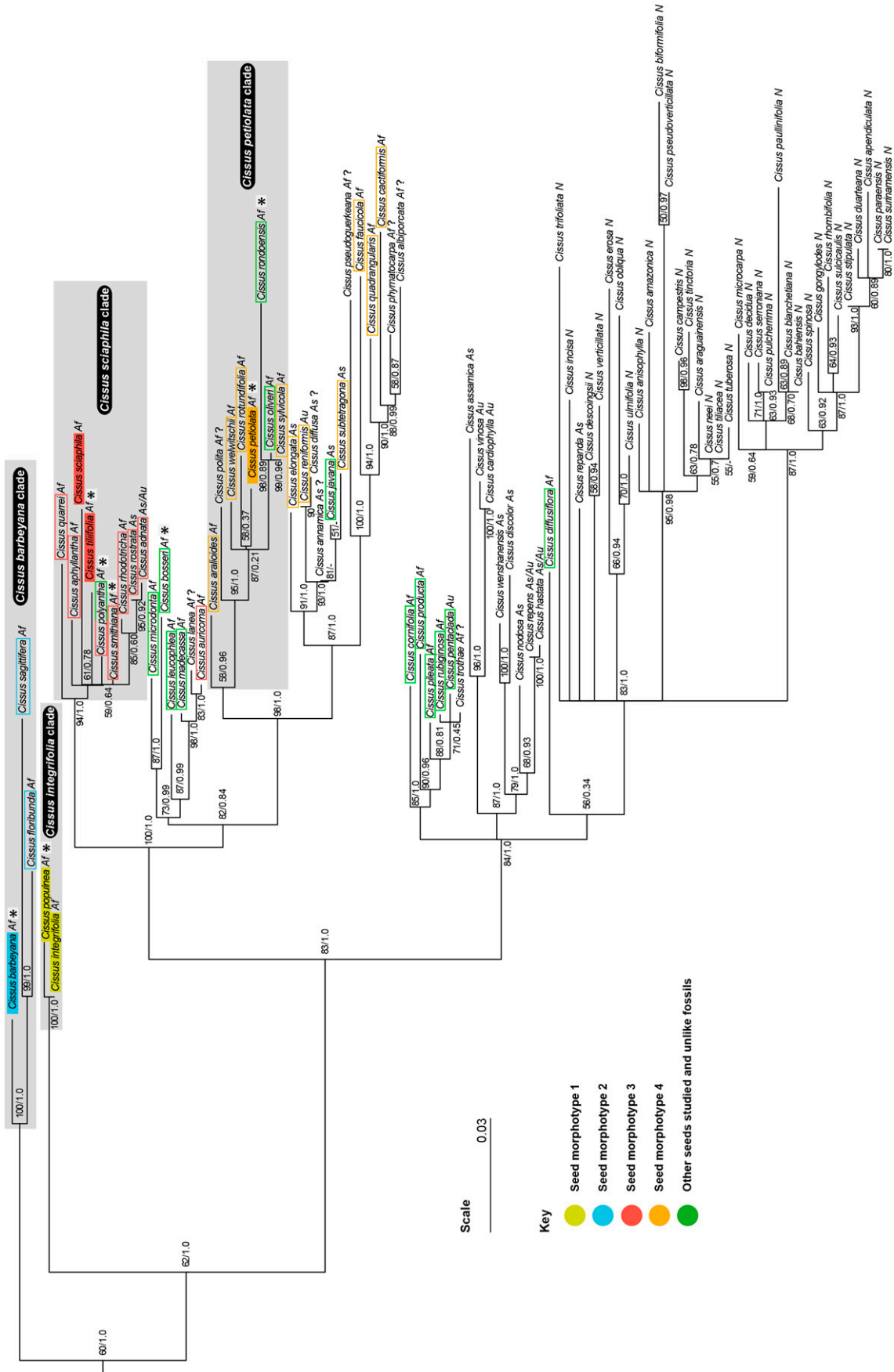
(Fig. 5). Seeds of *Cissus floribunda* (Fig. 6A) and *C. sagittifera* (fig. 14 of Descoings, 1967) also possess the morphotype 2 characters, (except that *C. sagittifera* lacks the ridged and faceted marginal area), suggesting that morphotype 2 is characteristic of the basal *Cissus barbeyana* clade and that *C. andrewsii* can be placed in this clade. Future work determining if *Cissus dasyantha* is in the *C. barbeyana* clade would test this hypothesis.

Morphotype 3—*Cissus rusingensis* has slightly laterally flattened seeds and ridges forming a complete to incomplete reticulum across the lateral faces. Extant species sharing these features (Table 1) include: *Cissus lebrunii* (fig. 13K of Dewit and Willems, 1960), *C. oreophila* (pl. 39, fig. 11 of Descoings, 1972), *C. sciaphila* (Fig. 6H), *C. smithiana* (Fig. 6G), and *C. tiliifolia* (Fig. 7C and Verdcourt, 1993). *Cissus sciaphila* and *C. tiliifolia* are found together in the *C. sciaphila* clade (*C. lebrunii* did not amplify), with five other African species (*C. aphyllantha*, *C. polyantha*, *C. quarrei*, *C. rhodotricha*, *C. smithiana*) and the Asian/Australasian species, *C. adnata* and *C. rostrata* (Fig. 5). Seed descriptions suggest these species share most, if not all, of the external morphological features of morphotype 3 (online Appendix S4). *Cissus polyantha* seeds are very variable in surface orna-

mentation from smooth to extensively ridged (pl. 36, figs. 11 and 12 of Descoings, 1972; fig. 13H of Dewit and Willems, 1960), also seen in our sampling of two specimens (online Appendix S1). However, one illustration of a ridged specimen (fig. 13H of Dewit and Willems, 1960) falls into morphotype 3. Morphotype 3 is characteristic of almost all of the species belonging to the *Cissus sciaphila* clade (and occurs in at least one collection of *C. polyantha*). The fact that *Cissus rusingensis* also shares this morphotype suggests that it was an early Miocene member of this clade. In the *C. microdonta*-*C. auricoma* clade (Fig. 5), *C. auricoma* is the only species with morphotype 3 seeds, suggesting parallel evolution of seed morphology in this case. Further sampling of both DNA and seed morphology would be needed to evaluate this possible parallelism.

Morphotype 4—Seeds of *Cissus psilata* are subrounded with smooth lateral faces almost identical to seeds of extant *C. petiolata* (Table 1; Figs. 6M, 7D). *Cissus petiolata* is found in a clade with seven solely African species (Fig. 5): *C. aralioides*, *C. oliveri*, *C. polita*, *C. rondoensis*, *C. rotundifolia*, *C. sylvicola*, *C. welwitschii*. Of these, *Cissus aralioides* (Fig. 6L), *C. rotundifolia*, *C. sylvicola*, and *C. welwitschii* have morphotype 4 seeds (online Appendix S4). *Cissus oliveri*, with coarsely

FIGURE 5 Phylogenetic tree of core *Cissus* clade obtained using maximum likelihood criteria, implemented in RAXML (Stamatakis, 2014), based on plastid DNA sequence data of Vitaceae, with particular focus on genus *Cissus*. Bootstrap values and posterior probabilities are indicated at nodes. Clades and seed morphotypes referred to in the text are indicated; species placed in seed morphotypes based on internal and external morphology are shown with solid color highlight, and those tentatively placed in seed morphotypes based on external illustrations and descriptions are distinguished by colored outline; distribution ranges indicated after species name (Af, Africa; As, Asia; Au, Australia; N, neotropics); species for which new DNA sequences were produced are highlighted with an asterisk; species for which no data on seed morphology could be found are denoted by a question mark. Scale bar shows degree of genetic change (nucleotide substitutions per site) as distance on the phylogram.



pitted seeds and very strong radial and lateral ribs (Verdcourt, 1993), and *C. rondoensis*, with seeds bearing two to three, faint transverse ridges (Verdcourt, 1993), lack the smooth seed coat typical of morphotype 4. These two species occupy contrasting habitats to the rest of the clade (Table 2), so contrasting seed morphology may reflect different environmental pressures.

Extant species in the *Cissus pseudoguierkeana*-*C. albiporcata* clade, for which seed descriptions were available, also share seed morphotype 4: *C. faucicola* and *C. quadrangularis* have smooth seeds (online Appendix S4), and *C. cactiformis* also has the smooth seed coat (Verdcourt, 1993). Furthermore, the majority of species in the *Cissus elongata*-*C. subtetragona* clade (Fig. 5) share morphotype 4 characters (online Appendix S4). This evidence suggests that morphotype 4 occurs throughout the broader *Cissus petiolata*-*C. albiporcata* clade (Fig. 5) and that *C. psilata* belongs in this clade.

Further morphological and molecular analyses, with expanded geographic and taxonomic sampling (including those species that failed to amplify for this study), are needed to fully evaluate the systematic significance of these seed morphotypes. This study focused on modern African species to place the African Miocene fossils in context. On the basis of extant species that have morphologically comparable seeds and their phylogenetic position, species from four clades of *Cissus* (or from the ends of their stem lineages) were present during the early Miocene in East Africa. These species were related to the two early-diverging clades of core *Cissus* (the *Cissus integrifolia* and *C. barbeyana* clades) and two later-diverging clades with mainly African species today, the *C. sciaphila* clade and the *C. petiolata*-*C. albiporcata* clade (Fig. 6).

Fossil plant biology and ecology—Habit and habitat data (Table 2) for nearest living relatives of the fossil *Cissus* (Fig. 6) can be used to consider the likely paleobiology and paleoecology of the fossil plants. In the *Cissus integrifolia* clade, the plants are lianas or herbaceous climbers in wide-ranging habitats, from evergreen forest and woodland to bushland and savanna grassland. Members of the *Cissus barbeyana* clade are herbaceous to woody lianas and predominantly occupy rainforest, gallery and riverine forest fringes. Species in the *Cissus sciaphila* clade are also herbaceous to woody climbers in rainforests or are scrambling shrubs or woody climbers in drier deciduous forest and woodland. The extant species of the *Cissus aralioides*-*C. albiporcata* clade are herbaceous to woody lianas or climbing shrubs, a number of which are succulent (*C. aralioides*, *C. cactiformis*, *C. petiolata*, *C. quadrangularis*, *C. rotundifolia*, *C. sylvicola*). They occur in riverine forest and wooded savanna to rocky outcrops, xerophilic thickets in *Acacia* mixed bushland and grassland (Table 2). The two members of the *Cissus petiolata* subclade with different seeds (see previous section) also differ in their habitat preferences, being most often found in moist rainforests.

These modern ecologies suggest that a diversity of climbers (either herbaceous or woody or both) were present in the early Miocene on Rusinga Island. These climbers may have occupied gallery or riverine forest (*Cissus andrewsii* related to the *C. barbeyana* clade) and evergreen forest, through woodland to savanna (*C. rusingensis* related to the *C. sciaphila* clade and *C. crenulata* related to the *C. integrifolia* clade). The plant producing the *Cissus psilata* seeds may have been somewhat succulent and hence able to occupy arid habitats as well as riverine forest or savanna, based on the habitats of a number of related extant species in the *C. aralioides*-*C. albiporcata* clade.

DISCUSSION

Homology of the ventral surface in Vitaceae seeds—The current convention for descriptive terminology of Vitaceae seeds (Chen and Manchester, 2011) and fossil *Cissus* seeds (Manchester et al., 2012b) has been followed here (online Appendix S6) to allow for ease of comparison with their work. However, an alternative interpretation is possible, particularly for the strongly flattened seeds (e.g., Figs. 1A–L, 2A–D, 3, 6A–F), whereby the ventral surface incorporates both ventral and apical (sensu online Appendix S6) and the ventral grooves are short occupying less than half of the dimension of that surface. This alternative seed orientation is followed in all the floras to which we refer in this paper (i.e., the modern seed illustrations in Fig. 6 are all rotated 90° clockwise). These two alternative homologies would best be investigated by a developmental study.

***Cissus* origins, phylogeny, and Miocene diversity in Africa**—Relationships among genera in the Vitaceae are mostly comparable between our study and the most recent previous studies of *Cissus* (Liu et al., 2013, 2016; Rodrigues et al., 2014), with limited support for the backbone of the trees (but see Wen et al., 2013 and Zhang et al., 2015). *Cissus* species are found in three distinct clades in all analyses, identified by Rodrigues et al. (2014) as the *Cissus striata* clade (clade III of Liu et al., 2013), the *C. trianae* clade (clade V of Liu et al., 2013) and the core *Cissus* clade, which contains most of the species. As in Liu et al. (2013), the earliest-diverging clades comprise mainly African species, although this is more evident in our study in which the first branches are exclusively African species. This topology provides support for an African origin for the genus, as Liu et al. (2013) also concluded.

The new African fossils are entirely consistent with an African origin for *Cissus*. The notable similarities in seed morphology between extant *Cissus* species and Hiwegi Formation fossils across multiple seed morphotypes suggest the presence of four clades or members of their stem lineages, indicating diversity of *Cissus*, by the early Miocene in Africa. Based on the divergence times (online Appendix S9), it appears that all four clades originated much earlier than the ca. 18 Ma age of the Miocene fossils: 41.5 Ma (HPD 31.5–51.0 Ma) for the split of the *Cissus barbeyana* clade from the rest of core *Cissus*; 36.0 Ma (HPD 27.6–44.7 Ma) for the divergence of the *C. integrifolia* clade; 24.6 Ma (HPD 18.1–32.1 Ma) for the divergence of the *C. sciaphila* clade; and 22.8 Ma (HPD ca. 16.6–30.0 Ma) for the divergence of the *C. aralioides*-*C. albiporcata* clade. The time-calibrated phylogeny (online Appendix S9) therefore suggests that several ghost lineages of *Cissus* await discovery in the fossil record. The new African Miocene seeds, and those from the Oligocene of Peru (see *Comparison with other fossil Cissus* below), provide fossil evidence consistent with the suggested phylogenetic history of *Cissus*.

Comparison with other fossil *Cissus*—The fossil record of the grape family (Vitaceae) extends back to the latest Cretaceous or earliest Paleogene in central India (Manchester et al., 2013) and to the Paleogene in North America and Europe (e.g., Manchester, 1994; Fairon-Demaret and Smith, 2002; Chen and Manchester, 2007; Collinson et al., 2012). However, for *Cissus*, the oldest, and only other, currently recognized examples are from the late early Oligocene Belén flora of northern Peru (Manchester et al., 2012b). This flora contains two *Cissus* species: *Cissus willardii* Berry and *Cissus lombardii* Manchester, Chen, & Lott. *Cissus willardii* is small

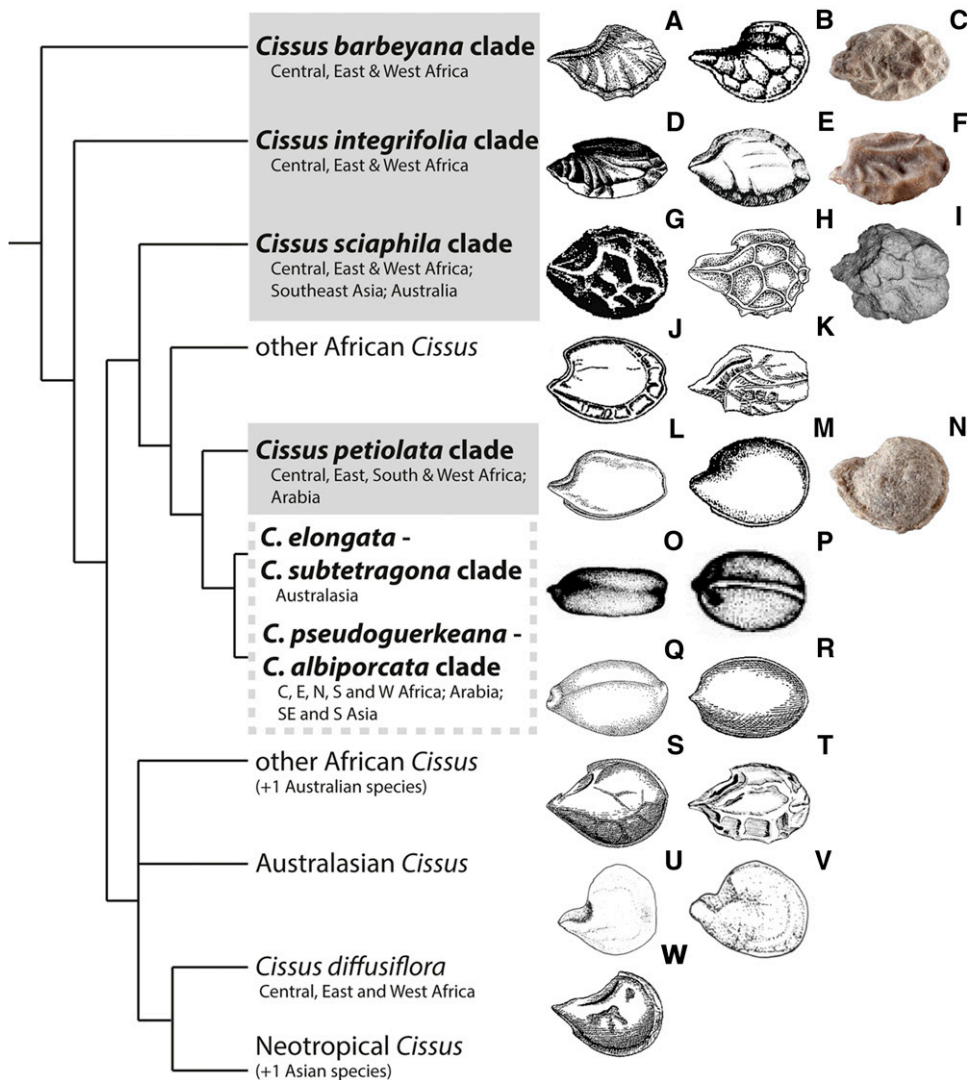


FIGURE 6 Major clades recognized in Fig. 5 with representative modern (A, B, D–E, G, H, J–M, O–W) and fossil (C, F, I, N) seed morphologies. Modern images all rotated 90° clockwise from the original source. Seed morphotype 1 (A–C) characterizes the *Cissus barbeyana* clade; morphotype 2 (D–F) the *C. integrifolia* clade; morphotype 3 (G–I) the *C. sciaphila* clade and morphotype 4 (L–N) the *C. petiolata* clade. Smooth seeds, somewhat similar to morphotype 4, also characterize the wider clade (in which the *C. petiolata* clade is basal) indicated by the dotted gray line. Sources of modern images are as follows: (A) *C. floribunda* (fig. 15.13: Descoings, 1967); (B) *C. barbeyana* (fig. 13E: Dewit and Willems, 1960); (D) *C. integrifolia* (fig. 13F: Dewit and Willems, 1960); (E) *C. populnea* (pl. 34, fig. 11: Descoings, 1972); (G) *C. smithiana* (pl. 52, fig. H: Dewit and Willems, 1960); (H) *C. sciaphila* (fig. 6.1c: Verdcourt, 1993); (J) *C. bosseri* (fig. 10.8: Descoings, 1967); (K) *C. leucophlea* (fig. 14.13: Descoings, 1967); (L) *C. aralioides* (fig. 13C: Dewit and Willems, 1960); (M) *C. petiolata* (fig. 13A: Dewit and Willems, 1960); (O) *C. elongata* (fig. 171.10: Chen et al., 2007); (P) *C. subtetragona* (fig. 171.2: Chen et al., 2007); (Q) *C. cactiformis* (fig. 9.8: Verdcourt, 1993); (R) *C. quadrangularis* (pl. 29, fig. 10: Descoings, 1972); (S) *C. cornifolia* (pl. 47, fig. 12 in Descoings, 1972); (T) *C. pileata* (fig. 13.9: Descoings, 1967); (U) *C. repens* (fig. 2B: Jackes, 1988); (V) *C. hastata* (fig. 5C: Jackes, 1988); (W) *C. diffusiflora* (pl. 44, fig. 11: Descoings, 1972). Seeds are not to scale and are all shown in lateral view, except (O) and (P), which are shown in apical view.

and globose with smooth lateral faces and large ventral infolds (fig. 2A–Q of Manchester et al., 2012b), unlike any of the fossils described above from Rusinga Island.

Conversely, *Cissus lombardii* shares some characteristics with African Miocene *C. crenulata* and modern *C. integrifolia* (seed mor-

photype 1), being bilaterally symmetrical, laterally flattened, elliptical in lateral view with a pronounced median perichalazal rib and a faintly faceted marginal area defined by a marginal ridge on each lateral face (fig. 3A–N of Manchester et al., 2012b). Thus, *Cissus lombardii* might be related to the *C. integrifolia* clade, extending its fossil record to the early Oligocene (30–28.5 Ma). However, *Cissus lombardii* is smaller in all dimensions than *C. crenulata* and *C. integrifolia* and lacks the distinct ornamenting ridges that cross the lateral faces in seeds of these species. The specimens of *Cissus lombardii* from the Belén flora are internal casts, which could result in a more subdued surface ornamentation than if the fossils were seeds themselves. However, as has been shown in extant *Cissus* seeds in this study using SRXTM (SRXTM videos of modern *Cissus* seeds are available from the Dryad Digital Repository, <http://dx.doi.org/10.5061/dryad.g9r36>), the inner surface of the endotesta closely parallels the outer surface, which would result in a similar pattern of ornamentation whether a fossil is an internal cast or a replacement of the endotesta itself. There is no indication of even faint ridges across the lateral faces in *Cissus lombardii* (fig. 3A and B of Manchester et al., 2012b), suggesting that the ornamentation of the original seed was significantly different from morphotype 1. The portion of the ventral surface containing the ventral infolds is “more or less planar (not markedly concave)” in *Cissus lombardii* (Manchester et al., 2012b, p. 936), rather than weakly to strongly concave as in *C. integrifolia* and *C. crenulata*. Therefore, *Cissus lombardii*, is clearly distinct from the African Miocene species.

Biogeographic implications—The position of previously unsampled modern African species near the base of the phylogeny (Fig. 5) reinforces the African origin for the core *Cissus* clade, suggested by Liu et al. (2013). The new African Miocene fossil *Cissus crenulata* has seed morphotype 1 as do both extant species of the *C. integrifolia* clade, confirming the presence of early-divergent members of the core *Cissus* clade in Africa by at least the Miocene.

The two modern species outside Africa in the *Cissus sciaphila* clade (*C. rostrata* and *C. adnata*) are advanced within the clade. Six of the seven modern African species in this clade are characterized by seeds of morphotype 3, and the seventh includes specimens with this

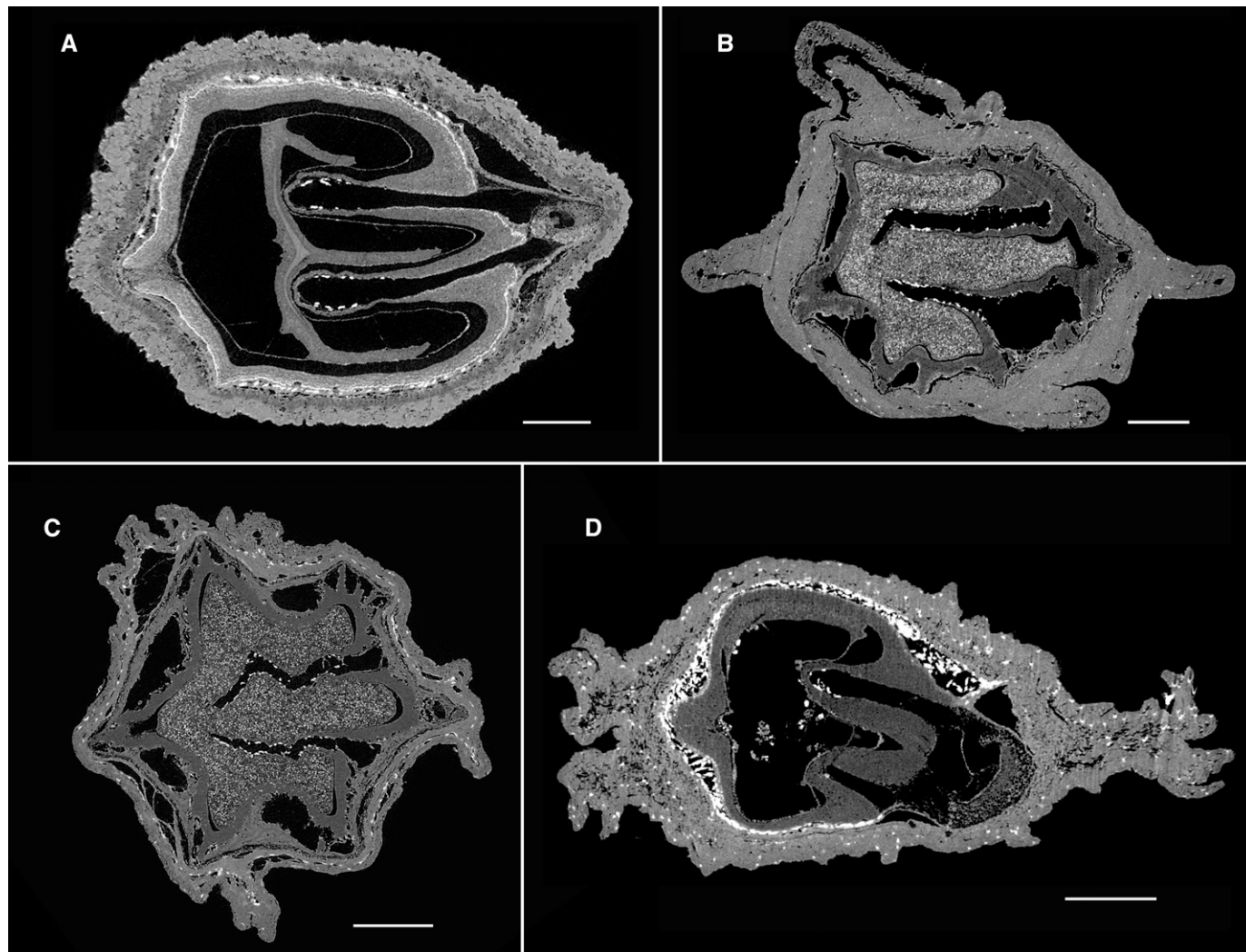


FIGURE 7 Digital transverse sections, produced by synchrotron-based X-ray tomographic microscopy, through fruits of modern African *Cissus*, using representative specimens to illustrate typical features of each seed morphotype listed in Table 1. (A) Morphotype 1, *Cissus integrifolia* Guill. & Perr. (B) Morphotype 2, *Cissus dasyantha* Gilg & M.Brandt. (C) Morphotype 3, *Cissus tiliifolia* Planch. (D) Morphotype 4, *Cissus petiolata* Hook.f. Transverse sections were obtained from near ventral part of fruits to best show features of ventral infolds and characteristics of seed coat layers. Scale bars = 1 mm.

seed morphotype. The new African Miocene fossil *Cissus rusingensis* also has seeds of morphotype 3. These data suggest that this clade originated in Africa. Dispersal during or after the Neogene to Australasia resulted in the modern pantropical intercontinental disjunct distribution. The calibrated phylogeny presented here (online Appendix S9) suggests that the divergence of Australasian species occurred near the end of the Pliocene at 2.7 Ma (HPD 0.8–5.5 Ma) differing from, although within the error of, the late Miocene estimate of 7.8 Ma (HPD 3.0–15.1 Ma) made by Liu et al. (2013).

Liu et al. (2013) argued that transoceanic long-distance dispersal, rather than terrestrial mammalian dispersal, was the most likely explanation for pantropical intercontinental disjunctions in *Cissus* because *Cissus* fruits are fleshy and, although in some instances dispersed by mammals, are predominantly bird-dispersed, enabling long-distance transport by bird migration. Multiple large islands across the Indian Ocean may have facilitated an out-of-Africa migration by acting as migratory “stepping stones”, as invoked for dispersal of other vitaceous genera (e.g., *Cayratia*; Lu et al., 2013).

The distributions of modern species in all four clades containing nearest living relatives to the fossils extend across Africa from East to West (Table 2). The fossil seeds suggest that the clades containing these living relatives may have had their origins in East Africa with subsequent spread to the rest of the continent. However, additional African fossil records of *Cissus* are needed to document dispersal patterns.

Paleoenvironmental implications—Previous paleoenvironmental reconstructions from the Hiwegi Formation have inferred a habitat mosaic inhabited by early hominoids, such as *Ekembo* (see McNulty et al., 2015). Evidence for mosaic habitats comes from gastropod (Verdcourt, 1963; Pickford, 1995) and mammal faunas (e.g., Andrews and Van Couvering, 1975), paleosols (Retallack et al., 1995) and paleobotany (Collinson et al., 2009; Maxbauer et al., 2013; Michel et al., 2014). Collinson et al. (2009) concluded that the overall paleoenvironmental signal, considering the evidence from plants, mammals, gastropods and paleosols, was one of “mixed habitats

dominated by woodlands, with waterside environments and small patches of forest big enough to support forest faunas” (p. 161). This conclusion is very similar to that derived from the possible fossil *Cissus* paleoecologies based on nearest living relatives (see *Fossil plant paleobiology and paleoecology*).

The vegetation in which *Cissus andrewsii*, *C. crenulata*, and *C. psilata* lived cannot be inferred from associated fossils, as the specimens were surface-picked. However, the context of the *Cissus rusingensis* fossils is well understood as they derive from in situ excavations of plant litter assemblages at the R117 site (Collinson et al., 2009). These litter assemblages were interpreted to have accumulated under a continuous canopy in deciduous, broad-leaved woodland bordering a river, based on the fossil fruits and seeds and their taphonomy (Collinson et al., 2009). *Cissus rusingensis* is therefore known to have inhabited a closed riverine woodland, consistent with interpretations made for this species from inferred near living relatives.

Recent studies have revealed temporal paleoenvironmental changes through the Hiwegi Formation (Michel et al., 2013, 2014; Garrett et al., 2015) and have suggested that interpretations of mosaic paleoenvironments may be based on time-averaged faunal and floral assemblages that conflate separate, more homogeneous habitats. These studies suggest that more open, drier woodland habitats low in the Hiwegi Formation (e.g., Grit Member) gave way to dense, closed canopy forest further up (e.g., Fossil Bed and Kibanga Members), with early hominoid fossils recovered from both paleoenvironments (Garrett et al., 2015). Since the stratigraphic context of *Cissus andrewsii*, *C. crenulata*, and *C. psilata* are unknown and they are not associated with *C. rusingensis*, the four new species of *Cissus* described may or may not have existed contemporaneously. Despite this uncertainty, it is known from in situ excavations in the Fruit and Nut Bed (Collinson et al., 2009) and stratigraphically associated leaf assemblages (Maxbauer et al., 2013) that a riverine mosaic habitat of woodland and forest existed during the deposition of the Grit Member of the lower Hiwegi Formation. The paleoecology of the new fossil species of *Cissus*, inferred from living relatives and supported (for *Cissus rusingensis*) by associated fossils, provides new evidence for mosaic landscapes on Rusinga Island during the early Miocene, ranging from gallery or riverine forest to woodland, bushland, and savanna.

ACKNOWLEDGEMENTS

N.F.A. thanks the Palaeontological Association for the award of an Undergraduate Research Bursary (PA-UB201401), which supported this work. M.K.B. thanks the Palaeontological Scientific Trust, South Africa (PAST) for funding a modern plant reference collection. Fieldwork in Kenya in 1981–1982 was undertaken with permission granted by the Office of the President of Kenya in cooperation with Richard Leakey, then Director of the National Museums of Kenya, Nairobi (KNM). M.E.C. thanks the University of London Central Research Fund for funding fieldwork in 1981–1982. The authors thank the Leakey Foundation for financial support to M.E.C. in 1980–1982 and M.K.B. in 2005–2006. They also thank the Royal Botanic Gardens, Kew; the Botanic Garden Meise, Belgium; the National Museums of Kenya, Nairobi (KNM); and the Natural History Museum, London (NHMUK), for access to specimens. The SRXTM work was performed on the TOMCAT beamline at the Swiss Light Source (SLS), Paul Scherrer Institut, Switzerland. They also thank the NHMUK for use of their μ CT and VP-SEM facilities and fossil macrophotography, Sven Landrein for logistical support at

Kew Herbarium and Peta Hayes for curatorial assistance at NHMUK. Steven Manchester and one anonymous reviewer are thanked for their helpful and extensive comments, which considerably improved the manuscript.

LITERATURE CITED

- Adams, N. F., M. E. Collinson, S. Y. Smith, M. K. Bamford, F. Forest, P. Malakasi, F. Marone, and D. Sykes. 2016. Data from: X-rays and virtual taphonomy resolve the first *Cissus* (Vitaceae) macrofossils from Africa as early diverging members of the genus. Dryad Digital Repository. doi:10.5061/dryad.g9r36
- Andrews, A. L., D. J. Peppe, K. P. McNulty, W. E. H. Harcourt-Smith, H. M. Dunsworth, A. L. Deino, and D. L. Fox. 2009. Magnetostratigraphy of the Early Miocene Kulu and Hiwegi Formations on Rusinga Island (Lake Victoria, Kenya). *Geological Society of America Abstracts with Programs* 41: 672.
- Andrews, P. 1992. Community evolution in forest habitats. *Journal of Human Evolution* 22: 423–438.
- Andrews, P., and E. Simons. 1977. A new African Miocene gibbon-like genus, *Dendropithecus* (Hominoidea, Primates) with distinctive postcranial adaptations: Its significance to origin of Hylobatidae. *Folia Primatologica* 28: 161–169.
- Andrews, P., and J. H. Van Couvering. 1975. Palaeoenvironments in the East African Miocene. In F. Szalay [ed.], *Contribution to primate paleobiology*, vol. 5, 62–103. Karger, Basel, Switzerland.
- Beentje, H. 1994. Kenya trees, shrubs and lianas. National Museums Kenya, Nairobi, Kenya.
- Bestland, E. A., G. D. Thackray, and G. J. Retallack. 1995. Cycles of doming and eruption of the Miocene Kisingiri volcano, southwest Kenya. *Journal of Geology* 103: 598–607.
- Butler, P. M. 1984. Macroscelidea, Insectivora and Chiroptera from the Miocene of East Africa. *Palaeovertebrata* 14: 117–200.
- Chen, I., and S. R. Manchester. 2007. Seed morphology of modern and fossil *Ampelocissus* (Vitaceae) and implications for phytogeography. *American Journal of Botany* 94: 1534–1553.
- Chen, I., and S. R. Manchester. 2011. Seed morphology of Vitaceae. *International Journal of Plant Sciences* 172: 1–35.
- Chen, Z., H. Ren, and J. Wen. 2007. Vitaceae. In C. Y. Wu, D.-Y. Hong, and P. H. Raven [eds.], *Flora of China*, vol. 12, 173–222. Science Press, Beijing, China and Missouri Botanical Garden Press, St. Louis, Missouri, USA.
- Chesters, K. I. M. 1957. The Miocene flora of Rusinga Island, Lake Victoria, Kenya. *Palaeontographica. Abteilung B, Paläophytologie* 101: 29–71.
- Chesters, K. I. M. 1958. Fossil angiosperms as indicators of early Tertiary conditions in Africa with special reference to the Miocene flora of Rusinga Island, Lake Victoria. PhD dissertation, University of Cambridge, Cambridge, UK.
- Clos, L. M. 1995. A new species of *Varanus* (Reptilia: Sauria) from the Miocene of Kenya. *Journal of Vertebrate Paleontology* 15: 254–267.
- Collinson, M. E., P. Andrews, and M. K. Bamford. 2009. Taphonomy of the early Miocene flora, Hiwegi Formation, Rusinga Island, Kenya. *Journal of Human Evolution* 57: 149–162.
- Collinson, M. E., M. K. Bamford, and S. Y. Smith. 2013. The Early Miocene fruit and seed floras from Rusinga and Mfwangano Islands, Kenya. *Geological Society of America Abstracts with Programs* 45: 457.
- Collinson, M. E., S. R. Manchester, and V. Wilde. 2012. Fruits and seeds of the Middle Eocene Messel biota, Germany. *Abhandlungen der Senckenberg Gesellschaft für Naturforschung* 570: 1–251.
- Conrad, J. L., K. Jenkins, T. Lehmann, F. K. Manthi, D. J. Peppe, S. Nightingale, A. Cossette, et al. 2013. New specimens of ‘*Crocodylus pigotti*’ (Crocodylidae) from Rusinga Island, Kenya, and generic reallocation of the species. *Journal of Vertebrate Paleontology* 33: 629–646.
- De Santo, A. V., A. Fioretto, G. Bartoli, and A. Alfani. 1987. Gas exchange of two CAM species of the genus *Cissus* (Vitaceae) differing in morphological features. *Photosynthesis Research* 13: 113–124.
- Descouings, B. 1967. Vitacées. In H. Humbert [ed.], *Flore de Madagascar et des Comores*, vol. 124, 1–151. Muséum National d’Histoire Naturelle, Paris, France.

- Descouings, B. 1972. Vitacées, Leeacées. In A. Aubréville and J.-F. Leroy [eds.], *Flore du Cameroun*, vol. 13, 1–132. Muséum National d'Histoire Naturelle, Paris, France.
- Dewit, J., and L. Willems. 1960. Vitaceae. In W. Robyns, P. Staner, F. Demaret, R. Germain, G. Gilbert, L. Hauman, M. Homès, et al. [eds.], *Flore du Congo belge et du Ruanda-Urundi. Spermatophytes*, vol. 9, 453–567. Institut National pour l'Étude Agronomique du Congo belge, Brussels, Belgium.
- Doyle, J. J., and J. L. Doyle. 1987. A rapid isolation procedure for small quantities of fresh leaf tissue. *Phytochemical Bulletin* 19: 11–15.
- Drake, R. E., J. A. Van Couvering, M. H. Pickford, G. H. Curtis, and J. A. Harris. 1988. New chronology for the Early Miocene mammalian faunas of Kisingiri, Western Kenya. *Journal of the Geological Society* 145: 479–491.
- Drummond, A. J., and A. Rambaut. 2007. BEAST: Bayesian evolutionary analysis by sampling trees. *BMC Evolutionary Biology* 7: 214.
- Edgar, R. C. 2004. MUSCLE: Multiple sequence alignment with high accuracy and high throughput. *Nucleic Acids Research* 32: 1792–1797.
- Fairon-Demaret, M., and T. Smith. 2002. Fruits and seeds from the Tienen Formation at Dormaal, Palaeocene-Eocene transition in eastern Belgium. *Review of Palaeobotany and Palynology* 122: 47–62.
- Garrett, N. D., D. L. Fox, K. P. McNulty, L. Michel, and D. J. Peppe. 2015. Early Miocene paleoenvironments of Rusinga Island, Kenya: New data from fossil mammalian tooth enamel stable isotope compositions. *Journal of Vertebrate Paleontology, Program with Abstracts* 2015: 130.
- GBIF [Global Biodiversity Information Facility]. 2013. GBIF data portal. Website <http://www.gbif.org> [accessed 02 October 2015].
- Harris, J., and J. Van Couvering. 1995. Mock aridity and the paleoecology of volcanically influenced ecosystems. *Geology* 23: 593–596.
- Harrison, C. J. O. 1980. Fossil birds from Afrotropical Africa in the collection of the British Museum (Natural History). *Ostrich* 51: 92–98.
- Harrison, T. 2002. Late Oligocene to middle Miocene catarrhines from Afro-Arabia. In W. Hartwig [ed.], *The primate fossil record*, 311–338. Cambridge University Press, Cambridge, UK.
- Harrison, T., and P. Andrews. 2009. The anatomy and systematic position of the early Miocene proconsulid from Meswa Bridge, Kenya. *Journal of Human Evolution* 56: 479–496.
- Hartman, J. H., and A. J. Kihm. 1995. Age of Meek and Hayden's Fort Union Group (Paleocene), Upper Missouri River, North Dakota-Montana. In L. D. Hunter and R. A. Schalla [eds.], *Proceedings of the 7th International Williston Basin Symposium*, 417–428. Montana Geological Society, Billings, Montana, USA.
- Jacks, B. R. 1988. Revision of the Australian Vitaceae, 3. *Cissus* L. *Austrobaileya* 2: 481–505.
- Janis, C. M. 1993. Tertiary mammal evolution in the context of changing climates, vegetation, and tectonic events. *Annual Review of Ecology and Systematics* 24: 467–500.
- Keay, R. W. J. 1958. Ampelidaceae. In R. W. J. Keay [ed.], *Flora of west tropical Africa*, vol. 1, part 2, 671–683. Crown Agents for Oversea Governments and Administrations, London, UK.
- Kihm, A. J., and J. H. Hartman. 1991. The age of the Sentinel Butte Formation, North Dakota. *Journal of Vertebrate Paleontology* 11: 40A.
- Le Gros Clark, W. E., and L. S. B. Leakey. 1951. The Miocene Hominoidea of East Africa. *Fossil Mammals of Africa, British Museum, Natural History* 1: 1–117.
- Leakey, L. S. B. 1952. Lower Miocene invertebrates from Kenya. *Nature* 169: 624–625.
- Liu, X.-Q., S. M. Ickert-Bond, L.-Q. Chen, and J. Wen. 2013. Molecular phylogeny of *Cissus* L. of Vitaceae (the grape family) and evolution of its pantropical intercontinental disjunctions. *Molecular Phylogenetics and Evolution* 66: 43–53.
- Liu, X.-Q., S. M. Ickert-Bond, Z.-L. Nie, Z. Zhou, L.-Q. Chen, and J. Wen. 2016. Phylogeny of the *Ampelocissus*-*Vitis* clade in Vitaceae supports the New World origin of the grape genus. *Molecular Phylogenetics and Evolution* 95: 217–228.
- Lombardi, J. A. 2000. Vitaceae: Géneros *Ampelocissus*, *Ampelopsis* e *Cissus*. *Flora Neotropica Monographs* 80: 1–250.
- Lu, F.-Y. 1993. Vitaceae. In T. C. Huang, C. F. Huang, Z. Y. Li, H. C. Lo, H. Ohashi, C. F. Shen, and C. J. Wang [eds.], *Flora of Taiwan*, vol. 3, 696–710. Committee of the Flora of Taiwan, Taipei, Taiwan.
- Lu, L., W. Wang, Z. Chen, and J. Wen. 2013. Phylogeny of the non-monophyletic *Cayratia* Juss. (Vitaceae) and implications for character evolution and biogeography. *Molecular Phylogenetics and Evolution* 68: 502–515.
- Manchester, S. R. 1994. Fruits and seeds of the middle Eocene Nut Beds flora, Clarno Formation, Oregon. *Palaeontographica Americana* 58: 1–205.
- Manchester, S. R., I. Chen, and T. A. Lott. 2012b. Seeds of *Ampelocissus*, *Cissus*, and *Leea* (Vitaceae) from the Paleogene of western Peru and their biogeographic significance. *International Journal of Plant Sciences* 173: 933–943.
- Manchester, S. R., F. Herrera, E. Fourtanier, J. Barron, and J.-N. Martinez. 2012a. Oligocene age of the classic Belén fruit and seed assemblage of north coastal Peru based on diatom biostratigraphy. *Journal of Geology* 120: 467–476.
- Manchester, S. R., D. K. Kapgate, and J. Wen. 2013. Oldest fruits of the grape family (Vitaceae) from the Late Cretaceous Deccan Cherts of India. *American Journal of Botany* 100: 1849–1859.
- Marone, F., B. Münch, and M. Stampanoni. 2010. Fast reconstruction algorithm dealing with tomography artifacts. *Proceedings of the Society for Photo-Instrumentation Engineers* 7804: 780410.
- Marone, F., and M. Stampanoni. 2012. Regridding reconstruction algorithm for real-time tomographic imaging. *Journal of Synchrotron Radiation* 19: 1029–1037.
- Maxbauer, D. P., D. J. Peppe, M. Bamford, K. P. McNulty, W. E. H. Harcourt-Smith, and L. E. Davis. 2013. A morphotype catalog and paleoenvironmental interpretations of early Miocene fossil leaves from the Hiwegi Formation, Rusinga Island, Lake Victoria, Kenya. *Palaeontologia Electronica* 16: 28A.
- McNulty, K. P., D. R. Begun, J. Kelley, F. K. Manthi, and E. N. Mbua. 2015. A systematic revision of *Proconsul* with the description of a new genus of early Miocene hominoid. *Journal of Human Evolution* 84: 42–61.
- McNulty, K. P., W. E. H. Harcourt-Smith, and H. M. Dunsworth. 2007. New primate fossils from Rusinga Island, Kenya. *American Journal of Physical Anthropology* 132 (Supplement): 170.
- Michel, L. A., D. J. Peppe, S. G. Driese, K. P. McNulty, D. L. Fox, and N. Garrett. 2013. Equatorial paleoenvironment leading into the Miocene Climatic Optimum: Lessons learned from Rusinga and Mfangano Islands, Lake Victoria Kenya. *Geological Society of America Abstracts with Programs* 45: 457.
- Michel, L. A., D. J. Peppe, J. A. Lutz, S. G. Driese, H. M. Dunsworth, W. E. H. Harcourt-Smith, W. H. Horner, et al. 2014. Remnants of an ancient forest provide ecological context for Early Miocene fossil apes. *Nature Communications* 5: 3236.
- Muller, J. 1981. Fossil pollen records of extant angiosperms. *Botanical Review* 47: 1–142.
- Nichols, D. J., and H. L. Ott. 1978. Biostratigraphy and evolution of the *Momipites-Caryapollenites* lineage in the early tertiary in the Wind River Basin, Wyoming. *Palynology* 2: 93–112.
- Nie, Z. L., H. Sun, S. R. Manchester, Y. Meng, Q. Luke, and J. Wen. 2012. Evolution of the intercontinental disjunctions in six continents in the *Ampelopsis* clade of the grape family (Vitaceae). *BMC Evolutionary Biology* 12: 17.
- Peppe, D. J., A. L. Deino, K. P. McNulty, T. Lehmann, W. E. H. Harcourt-Smith, H. M. Dunsworth, and D. L. Fox. 2011. New age constraints on the early Miocene faunas from Rusinga and Mfangano Islands (Lake Victoria, Kenya). *American Journal of Physical Anthropology* 144 (Supplement): 237 [abstract].
- Pickford, M. 1981. Preliminary Miocene mammalian biostratigraphy for western Kenya. *Journal of Human Evolution* 10: 73–97.
- Pickford, M. 1995. Fossil land snails of East Africa and their palaeoecological significance. *Journal of African Earth Sciences* 20: 167–226.
- Pickford, M. 2002. Palaeoenvironments and hominoid evolution. *Zeitschrift für Morphologie und Anthropologie* 83: 337–348.
- Pickford, M., B. Senut, D. Gommery, and E. Musiime. 2009. Distinctiveness of *Ugandapithecus* from *Proconsul*. *Estudios Geológicos* 65: 183–241.
- Reed, K. E. 1997. Early hominid evolution and ecological change through the African Plio-Pleistocene. *Journal of Human Evolution* 32: 289–322.

- Retallack, G. J., E. A. Bestland, and D. P. Dugas. 1995. Miocene paleosols and habitats of *Proconsul* on Rusinga Island, Kenya. *Journal of Human Evolution* 29: 53–91.
- Rich, P. V., and C. A. Walker. 1983. A new genus of Miocene flamingo from East Africa. *The Ostrich* 54: 95–104.
- Robinson, J. T. 1963. Adaptive radiation in the australopithecines and the origin of man. In F. C. Howell and F. Bourliere [eds.], African ecology and human evolution, 385–416. Aldine, Chicago, Illinois, USA.
- Rodrigues, J. G., J. A. Lombardi, and M. B. Lovato. 2014. Phylogeny of *Cissus* (Vitaceae) focusing on South American species. *Taxon* 63: 287–298.
- Salard-Cheboldaëff, M. 1978. Sur la palynoflore Maestrichtienne et Tertiaire du bassin sédimentaire littoral du Cameroun. *Pollen et Spores* 20: 215–260.
- Salard-Cheboldaëff, M. 1981. Palynologie Maestrichtienne et Tertiaire du Cameroun. Resultats botaniques. *Review of Palaeobotany and Palynology* 32: 401–439.
- Shaw, J., E. B. Lickey, J. T. Beck, S. B. Farmer, W. Liu, J. Miller, K. C. Siripun, et al. 2005. The tortoise and the hare II: Relative utility of 21 noncoding chloroplast DNA sequences for phylogenetic analysis. *American Journal of Botany* 92: 142–166.
- Smith, S. Y., M. E. Collinson, P. J. Rudall, D. A. Simpson, F. Marone, and M. Stampanoni. 2009. Virtual taphonomy using SRXTM reveals cryptic features and internal structure of modern and fossil plants. *Proceedings of the National Academy of Sciences, USA* 106: 12013–12018.
- Stamatakis, A. 2014. RAxML version 8: A tool for phylogenetic analysis and post-analysis of large phylogenies. *Bioinformatics* 30: 1312–1313.
- Stampanoni, M., A. Groso, A. Isenegger, G. Mikuljan, Q. Chen, A. Bertrand, S. Henein, et al. 2006. Trends in synchrotron-based tomographic imaging: The SLS experience. *Proceedings of the Society for Photo-Instrumentation Engineers* 6318: 63180M.
- Taberlet, P., L. Gielly, G. Pautou, and J. Bouvet. 1991. Universal primers for amplification of three non-coding regions of chloroplast DNA. *Plant Molecular Biology* 17: 1105–1109.
- Thackray, G. D. 1994. Fossil nest of sweat bees (Halictinae) from a Miocene paleosol, Rusinga Island, western Kenya. *Journal of Paleontology* 68: 795–800.
- Verdcourt, B. 1963. The Miocene non-marine Mollusca of Rusinga Island, Lake Victoria, and other localities in Kenya. *Palaeontographica. Abteilung A, Paläozoologie, Stratigraphie* 121: 1–37.
- Verdcourt, B. 1993. Vitaceae. In R. M. Polhill [ed.], Flora of tropical east Africa, vol. 195, 1–149. A. A. Balkema, Rotterdam, Netherlands.
- Walker, A., and M. F. Teaford. 1988. The Kaswanga primate site: An Early Miocene hominoid site on Rusinga Island, Kenya. *Journal of Human Evolution* 17: 539–544.
- Walker, A., M. F. Teaford, L. Martin, and P. Andrews. 1993. A new species of *Proconsul* from the early Miocene of Rusinga/Mfangano Islands, Kenya. *Journal of Human Evolution* 25: 43–56.
- Wen, J., Z. Xiong, Z.-L. Nie, L. Mao, Y. Zhu, X.-Z. Kan, S. M. Ickert-Bond, et al. 2013. Transcriptome sequences resolve deep relationships of the grape family. *PLoS One* 8: e74394.
- Werdelin, L. 2011. A new genus and species of Felidae (Mammalia) from Rusinga Island, Kenya, with notes on early Felidae of Africa. *Estudios Geológicos* 67: 217–222.
- Whitworth, T. 1958. Miocene ruminants of East Africa. *Fossil Mammals of Africa, British Museum, Natural History* 15: 1–50.
- Wild, H., and R. B. Drummond. 1966. Vitaceae. In A. W. Exell, A. Fernandes, and H. Wild [eds.], Flora zambesiaca, vol. 2, part 2, 439–492. Crown Agents for Oversea Governments and Administrations, London, UK.
- Yeo, C. K., W. F. Ang, A. F. S. L. Lok, and K. H. Ong. 2012. Conservation status of *Cissus* L. (Vitaceae) of Singapore: With a special note on *Cissus repens* Lam. *Nature in Singapore* 5: 319–330.
- Zetter, R., M. J. Farabee, K. B. Pigg, S. R. Manchester, M. L. DeVore, and M. D. Nowak. 2011. Palynoflora of the Late Paleocene silicified shale at Almont, North Dakota, USA. *Palynology* 35: 179–211.
- Zhang, N., J. Wen, and E. A. Zimmer. 2015. Congruent deep relationships in the grape family (Vitaceae) based on sequences of chloroplast genomes and mitochondrial genes via genome skimming. *PLoS One* 10: e0144701.

APPENDIX 1 Voucher information and GenBank accession numbers of *Cissus* species, for which new sequences were produced for the present phylogenetic analysis.

Taxon; *trnL-F*; *rps16*; *trnC-petN*; *atpB-rbcL*; voucher information; Kew DNA Bank accession number.

Cissus barbeyana De Wild. & T.Durand; KX131178; -; -; Lisowski, S. 16406 (K); 31957. *Cissus bosseri* Desc.; KX131174; -; -; KX131172; Phillipson, P.B. & Rabesihanaka, S. 3140 (K); 31965. *Cissus petiolata* Hook.f.; KX131175; -; -; Luke, P.A. & WRQ 9365 (K); 31952. *Cissus*

polyantha Gilg & M.Brandt; KX131176; -; -; Deighton, F.C. 5208 (K); 31955. *Cissus populnea* Guill. & Perr.; KX131179; -; -; Daramola, B.O. 221 (K); 31968. *Cissus rondoensis* Verdc.; -; -; KX131170; Bidgood, S., Abdallah, R. & Vollesen, K. 1553 (K); 31961. *Cissus smithiana* (Baker) Planch.; KX131177; -; -; Louis, J. 559 (K); 31959. *Cissus tiliifolia* Planch.; KX131173; -; -; KX131171; Eilu, G. 240 (K); 31964.

APPENDIX 2 Species included in the phylogenetic analysis of family Vitaceae for which sequences were obtained from GenBank, with a particular focus on genus *Cissus*.

Taxon; *trnL-F*; *rps16*; *trnC-petN*; *atpB-rbcL*.

Cissus adnata Roxb.; JX476858; JX476547; JX476673; JX476429. *Cissus albiporcata* Masinde & L.E. Newton; JF437304; JX476548; JF437201; JX476430. *Cissus amazonica* Lindel; JX476859; JX476549; JX476674; JX476431. *Cissus anisophylla* Lombardi; AB235010; JX476550; JX476675; JX476432. *Cissus annamica* Gagnep.; -; -; JX476676; -. *Cissus antarctica* Vent.; JX476860; JX476551; JX476677; JX476433. *Cissus apendiculata* Lombardi; JX313413; -; -; -. *Cissus aphyllantha* Gilg; JX476862; JX476553; JX476679; JX476435. *Cissus araguainensis* Lombardi; JX313415; -; -; -. *Cissus aralioides* (Welw. ex Baker) Planch.; JF437305; -; JF437202; -. *Cissus assamica* (M.A. Lawson) Craib; JF437307; JX476559; JF437204; JX476441. *Cissus auricoma* Desc.; JX476866; JX476560; JX476682; JX476442. *Cissus bahiensis* Lombardi; JX313416; -; -; -. *Cissus biformifolia* Standl.; -; JX476562; JX476684; JX476444. *Cissus blanchetiana* Planch.; JX313417; -; -; -. *Cissus cactiformis* Gilg; JX476868; JX476563; JX476685; JX476445. *Cissus campestris* (Baker) Planch.; JX313418; -; -; -. *Cissus cardiophylla* Standley; EF179080; -; -; -. *Cissus cornifolia* (Baker) Planch.; JF437308; JX476567; JF437205; JX476449. *Cissus decidua* Lombardi; JX313419; -; -; -. *Cissus descoingsii* Lombardi; JX313420; -; -; -. *Cissus diffusa* (Miq.) Amshoff; JX476871; JX476569; JX476689; JX476451. *Cissus diffusiflora* (Baker) Planch.; JX476872; JX476570; -; JX476452. *Cissus discolor* Blume; JF437309; -; JF437206; -. *Cissus duarteana* Cambess.; JX313421; -; -; -. *Cissus elongata* Roxb.; -; JX476573; JX476691; JX476455. *Cissus erosa* Rich.; HM585942; HM585802; JX476693; HM585526. *Cissus faucicola* Wild & R.B.Drumm.; JX476874; JX476576; JX476694; JX476458. *Cissus floribunda* (Baker) Planch.; JX476875; JX476577; JX476695; JX476459. *Cissus gongyloides* (Burch. ex Baker) Planch.; JX476877; JX476579; JX476697; JX476461. *Cissus granulosa* Ruiz & Pav.; JX476880; JX476582; JX476700; JX476464. *Cissus hastata* Miq.; AB235012; -; JX476701; JX476465. *Cissus hypoglauca* Durras; JX476881; JX476583; JX476702; JX476466. *Cissus incisa* (Nutt.) Des Moul. Ex S.Watson; HM585944; HM585804; -; HM585528. *Cissus integrifolia* (Baker) Planch.; JX476882; JX476584; JX476703; JX476467. *Cissus javana* DC.; JX476883; JX476585; JX476704; JX476468. *Cissus lanea* Desc.; JX476884; JX476586; JX476705; JX476469. *Cissus leucophleus* (Scott-Elliott) Suess.; JX476885; JX476587; JX476706; JX476470. *Cissus madecassa* Desc.; JX476886; JX476588; JX476707; JX476471. *Cissus microcarpa* Vahl; JX476888; JX476590; JX476709; JX476473. *Cissus microdonta* Vahl; JX476889; JX476591; JX476710; JX476474. *Cissus neei* Croat; JX313424; -; -; -. *Cissus nodosa* Blume; HM585945; JX476592; JX476711; JX476475. *Cissus obliqua* Ruiz & Pav.; JX476890; JX476593; JX476712; JX476476. *Cissus oblonga* (Benth.) Planch.; EF179083; -; -; -. *Cissus oliveri* Gilg. ex Engl.; JX476892; JX476595; JX476714; JX476478. *Cissus paraensis* Lombardi; JX313427; -; -; -. *Cissus paullinifolia* Vell.; JX313426; -; -; -. *Cissus penninervis* (F.Muell.) Planch.; AF300300; -; -; -. *Cissus pentaclada* Jackes; EF179084; -; -; -. *Cissus phymatocarpa* Masinde & L.E. Newton; JF437311; JX476596; JF437209; JX476479. *Cissus pileata* Desc.; JX476893; JX476597; JX476715; JX476480. *Cissus polita* Desc.; JX476894; JX476598; JX476716; JX476481.

Cissus producta Afzel.; JF437312; JX476600; JX476718; JX476483. *Cissus pseudoguerekeana* Verdc.; JX476896; JX476601; JX476719; JX476484. *Cissus pseudovorticillata* Verdc.; JX476897; JX476602; JX476720; JX476485. *Cissus pulcherrima* Vell.; JX313429; -; -; -. *Cissus quadrangularis* L.; JF437313; JX476603; JF437211; JX476486. *Cissus quarrei* Dewit; JX476899; JX476605; JX476722; JX476488. *Cissus reniformis* Domin; EF179086; -; -; -. *Cissus repanda* Vahl; JX476900; JX476607; JX476724; JX476490. *Cissus repens* Lam.; HM585946; -; -; HM585530. *Cissus rhodotricha* (Baker) Desc.; JX476902; JX476609; JX476727; JX476492. *Cissus rhombifolia* Vahl; JX476905; JX476612; JX476729; JX476495. *Cissus rostrata* Korth.ex Planch.; AB235016; -; JX476731; JX476497. *Cissus rotundifolia* (Forssk.) Vahl; JF437315; JX476614; JF437213; JX476498. *Cissus rubiginosa* Welw. ex Bak. Planch.; JX476907; JX476616; JX476732; JX476500. *Cissus sagittifera* Desc.; JX476908; JX476617; JX476733; JX476501. *Cissus sciaphila* Gilg; JF437316; JX476619; JF437214; JX476503. *Cissus serroniana* (Glaz.) Lombardi; JX313430; -; -; -. *Cissus simsiana* Roem. & Schult.; JX476910; JX476620; JX476734; JX476504. *Cissus spinosa* Cambess.; JX313435; -; -; -. *Cissus sterculiifolia* (F.Muell. ex Benth.) Planch.; EF179088; -; -; -. *Cissus stipulata* Vell.; JX313436; -; -; -. *Cissus striata* Ruiz & Pav.; AB235017; -; JX476747; -. *Cissus subtetragona* Planch.; JX476923; JX476635; JF437216; JX476519. *Cissus sulcicaulis* (Baker) Planch.; JX313438; -; -; -. *Cissus surinamensis* Desc.; JX313439; -; -; -. *Cissus sylvicola* Masinde & L.E. Newton; JX476924; JX476636; JX476751; JX476520. *Cissus tiliacea* Kunth; JX313440; -; -; -. *Cissus tinctoria* Mart.; JX313414; -; -; -. *Cissus trianae* Planch.; JX313441; -; -; -. *Cissus trifoliata* (L.) L.; JX476926; JX476639; JX476755; JX476524. *Cissus trothae* Gilg & M. Brandt; JF437318; JX476640; JF437217; JX476525. *Cissus tuberosa* Moc. & Sesse ex DC.; JX476927; JX476641; JX476756; JX476526. *Cissus tweediana* (Baker) Planch.; EF179089; -; -; -. *Cissus ulmifolia* (Baker) Planch.; JX476928; JX476642; JX476757; JX476527. *Cissus verticillata* (L.) Nicolson & C.E. Jarvis; JX476929; JX476643; JX476758; JX476528. *Cissus vinosa* Jackes; EF179090; -; -; -. *Cissus welwitschii* (Baker) Planch.; JX476934; JX476651; -; JX476537. *Cissus wenshanensis* C.L. Li; HM585949; -; -; HM585533. *Ampelocissus acapulcensis* (Kunth) Planch.; JF437281; JX476543; JF437172; -. *Ampelocissus africana* (Lour.) Merr.; JQ182553; JQ182603; -; JQ182448. *Ampelocissus ascendiflora* Latiff; -; JQ182583; -; JQ182430. *Ampelocissus costaricensis* Lundell; -; -; -; AB234911. *Ampelocissus elephantina* Planch.; HM585932; HM585792; -; HM585516. *Ampelocissus erdwendbergiana* Planch.; JF437282; JX476544; JF437173; -. *Ampelocissus filipes* Planch.; AB234982; -; -; -. *Ampelocissus gracilis* Planch.; AB234983; -; -; -. *Ampelocissus javalensis* (Seem.) W.D. Stevens & A. Pool; AB234984; -; -; -. *Ampelocissus obtusata* (Welw. ex Baker) Planch.; JQ182556; JQ182612; -; JQ182457. *Ampelocissus thyriflora* (Blume) Planch.; JQ182546; JQ182593; -; JQ182438. *Ampelopsis bodinieri* (H. Lév. & Vaniot) Rehder; JF437284; JX476545; JF437175; JX476427. *Ampelopsis cantoniensis* Planch.; HM585933; HM585793; JX476667; HM585517. *Ampelopsis chaffanjonii* (H.Lév.) Rehder; JF437286; -; -; -. *Ampelopsis cordata* Michx.; AB234997; -; JF437178; -. *Ampelopsis*

APPENDIX 2 *Continued*

- delavayana* Planch; HM223253; -; -; -. *Ampelopsis rubifolia* (Wall.) Planch; JF437293; JX476546; JF437186; JX476428. *Cayratia acris* F. Muell; EF179070; -; -; -. *Cayratia clematidea* (F.Muell.) Domin; EF179072; -; -; -. *Cayratia cordifolia* C.Y. Wu ex C.L. Li; HM585934; HM585794; JX476668; HM585518. *Cayratia debilis* (Baker)Suess; JF437296; -; -; -. *Cayratia eurynema* B.L.Burtt; EF179073; -; -; -. *Cayratia gracilis* (Guill. & Perr.)Suess; JF437297; -; -; -. *Cayratia imerinensis* (Baker) Desc.; HM585936; HM585796; JX476669; HM585520. *Cayratia japonica* (Thunb.) Gagnep.; HM585937; -; -; HM585521. *Cayratia maritima* Jackes; EF179074; -; -; -. *Cayratia mollissima* Gagnep.; HM585938; HM585798; JX476671; HM585522. *Cayratia pedata* Gagnep.; AB235005; -; -; -. *Cayratia saponaria* (Seem. ex Benth.) Domin; EF179075; -; -; -. *Cayratia trifolia* (L.) Domin; HM585940; -; -; JX476672; HM585524. *Cayratia triternata* (Baker) Desc.; HM585941; -; -; -. *Clematicissus angustissima* (F.Muell.) Planch; EF179091; -; -; -. *Clematicissus opaca* (F. Muell) Jackes & Rossetto; JX476935; JX476652; JX476767; JX476538. *Cyphostemma adenocaula* (A.Rich.)Wild & R.B.Drumm; JX476936; JX476653; JX476768; JX476539. *Cyphostemma bainesii* (Hook.f.) Desc.; AB235025; -; -; -. *Cyphostemma duparquetii* (Planch.) Desc.; JF437324; -; JF437222; -. *Cyphostemma horombense* Desc.; HM585950; -; -; -. *Cyphostemma jiguu* Verdc.; JX476937; JX476655; JX476769; JX476540. *Cyphostemma kilimandscharicum* (Gilg) Wild & R.B.Drumm; JF437327; -; -; -. *Cyphostemma mappia* (Lam.) Galet; AB235026; -; -; -. *Cyphostemma maranguense* (Gilg) Desc.; JF437329; -; JF437227; -. *Cyphostemma montagnacii* Desc.; AB235027; -; JF437228; -. *Cyphostemma simulans* (C.A. Sm.) Wild & R.B. Drumm; HM585952; -; -; HM585536. *Leea aculeata* Blume; AB235087; -; -; -. *Leea guineensis* G. Don; -; JX476657; JF437235; JX476541. *Leea indica* (Burm.f.) Merr; HM585953; -; JX476771; HM585537. *Leea macrophylla* Roxb. ex Hornem. & Roxb.; JF437335; JX476659; JF437237; -. *Leea spinea* Desc.; HM585955; -; -; -. *Nothocissus spicifera* (Griff.) Latiff; JF437336; JX476660; JF437239; -. *Parthenocissus chinensis* C.L. Li; HM223263; HM223320; JF437240; HM223373. *Parthenocissus henryana* (Hemsl.) Graebn. ex Diels & Gilg; HM223272; HM223329; JF437244; HM223383. *Parthenocissus heptaphylla* (Buckl.) Britton ex Small; HM223256; -; -; -. *Parthenocissus himalayana* Planch; AB235034; -; -; -. *Parthenocissus laetevirens* Rehder; HM223267; -; -; -. *Parthenocissus quinquefolia* (L.) Planch; HM223275; HM223332; JF437246; HM223386. *Parthenocissus suberosa* Hand.-Mazz; HM223273; HM223330; JF437247; HM223384. *Parthenocissus tricuspidata* (Sieb. & Zucc.) Planch; HM223274; HM223331; JF437248; HM223385. *Parthenocissus vitacea* (Knerr) Hitchc; HM223295; -; -; -. *Pterisanthes eriopoda* Planch; -; JX476661; -; -; -. *Pterisanthes heterantha* M. Laws; AB235045; AB234965; -; AB234930. *Pterisanthes stonoi* Latiff; AB235046; JX476662; -; -; -. *Rhoicissus digitata* Gilg & Brandt; AB235047; -; -; -. *Rhoicissus rhomboidea* Planch; AB235049; -; -; -. *Rhoicissus tomentosa* (Lam.) Wild & R.B. Drumm; JF437342; JX476663; JF437251; -. *Rhoicissus tridentata* (L.f.) Wild & R.B. Drumm; JF437341; JX476664; JF437250; -. *Tetragium glabratum* Planch; HM585995; -; -; -. *Tetragium hemsleyanum* Diels & Gilg; HM586000; HM585860; -; HM585584. *Tetragium lanyuense* C.E. Chang; HM586009; HM585869; JF437257; HM585593. *Tetragium laxum* Merr; HM586017; -; -; -. *Tetragium lenticellatum* Planch; HM586019; -; -; -. *Tetragium loheri* Gagnep.; HM586021; -; -; -. *Tetragium obtectum* (Wall.) Planch; HM586029; HM585888; -; HM585614. *Tetragium pachyphyllum* (Hemsl.) Chun; HM586032; HM585891; JF437259; HM585616. *Tetragium petraeum* Jackes; EF179094; -; -; -. *Tetragium pyriforme* Gagnep.; HM586039; -; -; -. *Tetragium sichouense* C.L.Li; HM586047; -; -; -. *Tetragium triphyllum* (Gagnep.) W.T. Wang; HM586061; HM585919; -; HM585646. *Tetragium voinierianum* Pierre ex Gagnep; HM586067; -; -; -. *Vitis aestivalis* Michx. ; HM586070; HM585928; -; HM585655. *Vitis betulifolia* Diels & Gilg; JF437352; JX476665; JF437269; -. *Vitis flexuosa* Thunb; HM586071; HM585929; -; HM585656. *Vitis heyneana* Roem. & Schult; JF437354; JX476666; JF437273; -. *Vitis labrusca* L.; JX507364; JX507361; JX507362; JX507360. *Vitis mengziensis* C.L. Li; HM223276; HM223333; JF437270; HM223387. *Vitis popenoei* J.L. Fennell; HM586072; HM585930; JF437276; HM585657. *Vitis riparia* Michx; JF437357; -; JF437277; -. *Vitis rotundifolia* Michx; HM586073; HM585931; -; HM585658. *Vitis thunbergii* Siebold & Zucc.; AB235082; -; -; -. *Vitis vinifera* L.; -; -; -. *Vitis vulpina* L.; JQ182566; JQ182622; -; JQ182467. *Yua austro-orientalis* (F.P. Metcalf) C.L. Li; AB235085; -; -; -. *Yua thomsoni* (M.A. Lawson) C.L. Li; HM223277; HM223335; -; HM223389.